International Journal of *Geo-Information*

MDPI

Article

Spatiotemporal Changes and Trade-Offs/Synergies of Ecosystem Services in the Qin-Mang River Basin

Jiwei Zhao [1], Luyao Wang [1,*], Dong Jia [2] and Yaowen Wang [1]

[1] Water Conservancy College, North China University of Water Resources and Electric Power, Zhengzhou 450046, China; zhaojiwei@stu.ncwu.edu.cn (J.Z.); z202210010188@stu.ncwu.edu.cn (Y.W.)
[2] College of Civil Engineering and Transportation, North China University of Water Resources and Electric Power, Zhengzhou 450046, China; z202210030407@stu.ncwu.edu.cn
* Correspondence: z202210010075@stu.ncwu.edu.cn; Tel.: +86-152-3716-0597

Abstract: The Qin-Mang River Basin is an important biodiversity conservation area in the Yellow River Basin. Studying the spatiotemporal changes in its ecosystem services (ESs) and the trade-offs and synergies (TOSs) between them is crucial for regional ecological protection and high-quality development. This study, based on land use type (LUT), and meteorological and soil data from 1992 to 2022, combined with the InVEST model, correlation analysis, and spatial autocorrelation analysis, explores the impacts of land use/land cover changes (LUCCs) on ESs. The results show that: (1) driven by urbanization and economic development, the expansion of built-up areas has replaced cultivated land and forests, with 35,000 hectares of farmland lost, thereby increasing pressure on ESs; (2) ESs show an overall downward trend, habitat quality (HQ) has deteriorated, carbon storage (CS) remains stable but the area of low CS has expanded, and sediment delivery ratio (SDR) and water yield (WY) fluctuate due to human activities and climate influence; (3) the TOSs of ESs change dynamically, with strong synergies among HQ, CS, and SDR. However, in areas with water scarcity, the negative correlation between HQ and WY has strengthened; (4) spatial autocorrelation analysis reveals that in 1992, significant positive synergies existed between ESs in the northern and northwestern regions, with WY negatively correlated with other services. By 2022, accelerated urbanization has intensified trade-off effects in the southern and eastern regions, leading to significant ecological degradation. This study provides scientific support for the sustainable management and policymaking of watershed ecosystems.

Keywords: ecosystem services; trade-offs and synergies; spatial heterogeneity analysis; land use type transition; Qin-Mang River Basin

Academic Editors: Wolfgang Kainz, Jingzhe Wang, Yangyi Wu, Yinghui Zhang, Ivan Lizaga and Zipeng Zhang

Received: 1 October 2024
Revised: 24 December 2024
Accepted: 10 January 2025
Published: 19 January 2025

Citation: Zhao, J.; Wang, L.; Jia, D.; Wang, Y. Spatiotemporal Changes and Trade-Offs/Synergies of Ecosystem Services in the Qin-Mang River Basin. *ISPRS Int. J. Geo-Inf.* **2025**, *14*, 37. https://doi.org/10.3390/ijgi14010037

1. Introduction

Ecosystem services (ESs) refer to the direct and indirect benefits provided by natural ecosystems to human society through various pathways. As an essential support system for human survival and sustainable development, these services encompass multiple aspects, including resource supply and ecological regulation, and play an indispensable role in regional ecological security and global ecological stability [1,2]. However, with the intensification of climate change and the rapid development of human activities, approximately 60% of global ecosystems have undergone degradation, posing a severe threat to the stability and sustainability of ecosystems [3,4]. For instance, the shrinkage of wetlands not only leads to the deterioration of water quality but also significantly accelerates the loss of biodiversity [5,6]. This trend underscores the urgency of formulating scientifically sound ecological protection and management policies, the effectiveness of which depends on a comprehensive understanding of the dynamic changes in ESs and their interrelationships [7].

As one of the global biodiversity hotspots, China's ecosystems are under immense pressure from rapid urbanization and economic growth. Land use/land cover changes (LUCCs) have been widely recognized as the main drivers of dynamic changes in ESs [8]. In response to this challenge, the Chinese government has implemented ecological protection policies such as "Grain-for-Green" and "Ecological Protection Red Lines". These measures have alleviated ecological degradation to some extent, but regional imbalances between the supply and demand of ESs remain prominent, especially in ecologically fragile areas and regions undergoing rapid urbanization [9,10]. The Yellow River Basin, as a key ecological barrier in China, maintains a close relationship between the spatiotemporal dynamics of its ESs and human activities, making the study of ecosystem service changes in this area highly significant [11].

The Qin-Mang River Basin is located within the biodiversity conservation area of the Yellow River Basin and serves as a crucial part of the Yellow River wetlands with key ecological functions. Its unique geographical location makes it of vital importance to regional ecological protection. Existing studies primarily focus on the following aspects: water resource protection, biodiversity habitat quality (HQ), and the impacts of LUCCs on ESs. For example, previous studies have assessed the role of water resource management in watershed ecological stability through hydrological models, revealing the impacts of climate change and human activities on the water supply–demand balance [12]. Additionally, studies have explored the effects of LUCCs on HQ using biodiversity indicators, finding that urbanization significantly reduces HQ [13]. However, existing research lacks in-depth exploration of the trade-offs and synergies (TOSs) between ESs, especially regarding the systematic study of spatial heterogeneity and complex interaction mechanisms.

In response to the research gaps mentioned above, this study addresses the following scientific questions: (1) what spatiotemporal changes have occurred in ESs in the Qin-Mang River Basin over the past 30 years? (2) How have the TOSs between different ESs evolved? (3) How have LUCCs affected the spatiotemporal distribution of ESs? To address these questions, this study integrates land use type (LUT) data from 1992 to 2022, combined with the InVEST model, correlation analysis, and spatial autocorrelation analysis, to systematically evaluate the dynamic changes and spatiotemporal heterogeneity of ESs in the Qin-Mang River Basin and reveal the TOSs between these services. This study focuses on four main ESs: HQ, carbon storage (CS), sediment delivery ratio (SDR), and water yield (WY). These services were selected based on their importance for regional ecological security and their close relationship with LUCCs [14,15]. Through quantitative analysis, this study reveals the spatiotemporal dynamic characteristics of these ESs and explores the driving roles of urbanization and climate change on ESs.

The innovations of this study are reflected in the following aspects: (1) a systematic study of the dynamic changes in ESs in the Qin-Mang River Basin, an important ecological barrier region; (2) quantifying the TOSs between ESs using the InVEST model and spatial analysis methods; (3) a detailed analysis of the impact of LUCCs on the spatial heterogeneity and interaction mechanisms of ESs; (4) providing scientific support for optimizing regional land use planning and formulating ecological protection policies, contributing to the high-quality development of the Yellow River Basin. In conclusion, this study not only fills the research gap on ESs in the Qin-Mang River Basin but also provides important theoretical support and practical references for regional ecological protection and management.

2. Materials and Methods

2.1. Study Area

The Qin-Mang River Basin, located in the northwest of Henan Province, refers to the combined basin of the Qin River and its tributary, the Mang River, with a total area of approximately 306,240 hectares. This basin is a key energy and chemical industry base within the Yellow River Basin and is designated as the core area for the Ecological Protection and Restoration Project for the Mountains, Rivers, Forests, Farmlands, Lakes, Grasslands, and Deserts in the South Taihang region of Henan Province, playing a significant role as an ecological barrier. Geographically, the basin spans from 112°20′ to 113°39′ east longitude and from 34°49′ to 35°21′ north latitude. It connects the North China Plain with the Loess Plateau and is located between the second and third geomorphic steps (Figure 1). The climate in the region is classified as a warm, temperate semi-humid climate, with an average annual temperature of approximately 14.6 °C and an annual precipitation of about 641.7 mm, concentrated primarily in the summer months. The basin is rich in vegetation resources, home to 1609 species of higher plants, and supports several nationally protected species. According to the "Ecological Protection and Restoration Plan for Mountains, Rivers, Forests, Farmlands, Lakes, Grasslands, and Deserts in Henan Province", the Qin-Mang River Basin has been identified as a key area for ecological restoration, involving measures such as forest management, soil and water conservation, and wetland protection. The biodiversity and ESs in this region play a crucial role in ensuring regional ecological security.

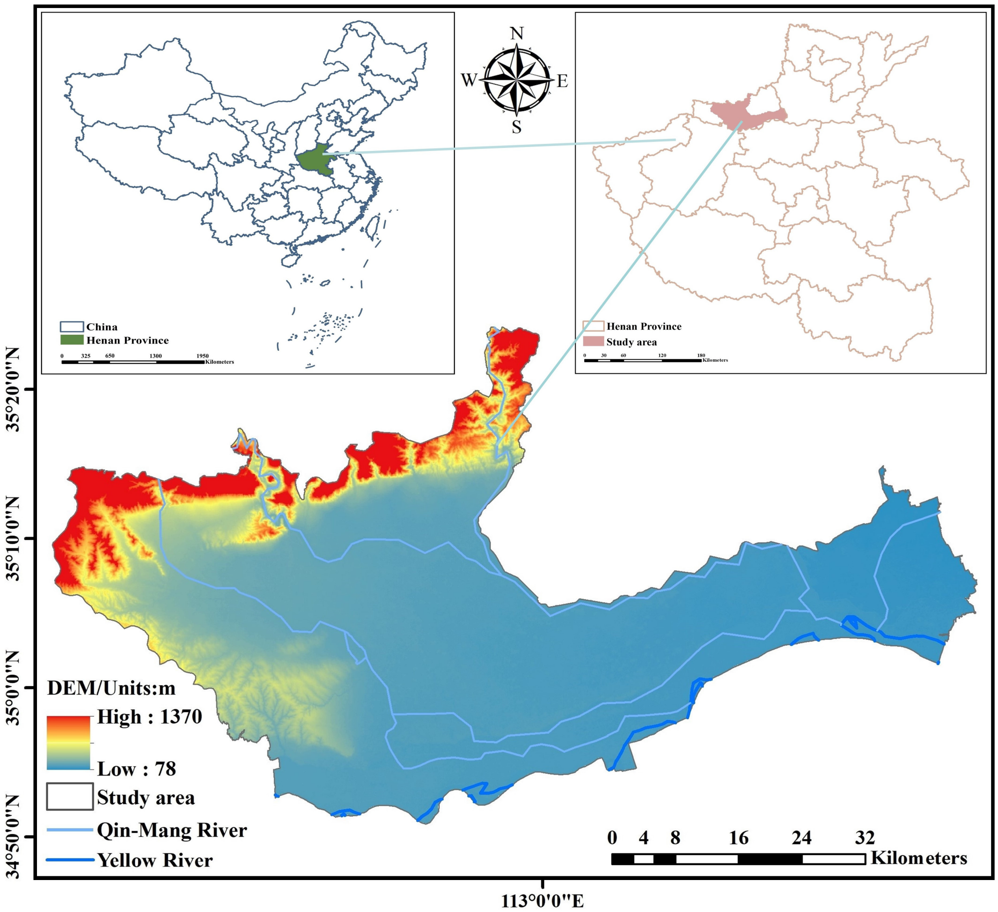

Figure 1. Geographic location and elevation map of the study area.

2.2. Data Sources and Preprocessing

This study's analysis is primarily based on LUT, Digital Elevation Model (DEM), administrative boundaries, natural environmental data, and socio-economic data. The selected datasets are intended to comprehensively reflect the ecological and socio-economic characteristics of the Qin-Mang River Basin and provide a reliable foundation for the research. Data sources and preprocessing steps are detailed in Table 1. During the data preprocessing phase, consistency in resolution and uniformity in the coordinate system across different datasets were ensured to enhance the accuracy and validity of the analysis results. All raster data were transformed into the WGS_1984_UTM_zone_49N coordinate system and processed to a uniform spatial resolution. Specific preprocessing steps included data clipping, resampling, reclassification, and spatial analysis operations.

Table 1. Main data sources.

Data Name	Resolution	Data Source	Data Preprocessing
DEM	90 m	Geospatial Data Cloud (http://www.gscloud.cn/, accessed on 13 July 2024)	The ArcGIS Clip tool was used to extract data for the study area and generate slope and aspect data.
LUCCs	30 m	Resource and Environment Science and Data Center (https://www.resdc.cn/, accessed on 19 July 2024)	The ArcGIS Reclassification tool was used to reclassify land use data into six categories based on the primary land classification standards and then clipped to the study area.
Precipitation, Temperature, and Potential Evapotranspiration Data	1 km	National Meteorological Science Data Centre (http://data.cma.cn, accessed on 30 July 2024)	Monthly data were processed in ArcGIS to obtain annual average data and then clipped to the study area.
Soil Type, Vegetation Type, and NDVI	1 km	The National Tibetan Plateau Data Center (http://data.tpdc.ac.cn/zh-hans/, accessed on 5 August 2024)	Data were clipped to the study area using ArcGIS.
Nighttime Light Index, GDP, and Population	1 km	Resource and Environment Science and Data Center (https://www.resdc.cn/, accessed on 2 August 2024)	Data were clipped to the study area using ArcGIS.
Railway, Water System, and Administrative Boundary Vector Data	-	National Catalogue Service for Geographic Information (https://www.webmap.cn/, accessed on 10 July 2024)	The ArcGIS Clip tool was used to extract the study area, and the Euclidean Distance tool was applied to calculate the distance to railways and water systems.

2.3. Research Methods

This study established a comprehensive analysis framework to systematically assess the impact of LUCCs on ESs in the Qin-Mang River Basin from 1992 to 2022, with a focus on revealing the TOSs between ESs and their spatial characteristics. Through the land use transfer matrix, this study quantified LUT transformation characteristics and rates at different time periods, analyzing the driving forces of urbanization and economic development on natural land. Coupled with the InVEST model, this study quantified the spatiotemporal dynamics of key ESs such as HQ, CS, SDR, and WY, providing data support for understanding the impact of LUCCs on ESs. Correlation analysis was used to reveal the TOSs between ESs, and bivariate local Moran's I (BLI) was employed to analyze their spatial clustering and dispersion, identifying key hotspot and coldspot areas. The research framework is shown in Figure 2.

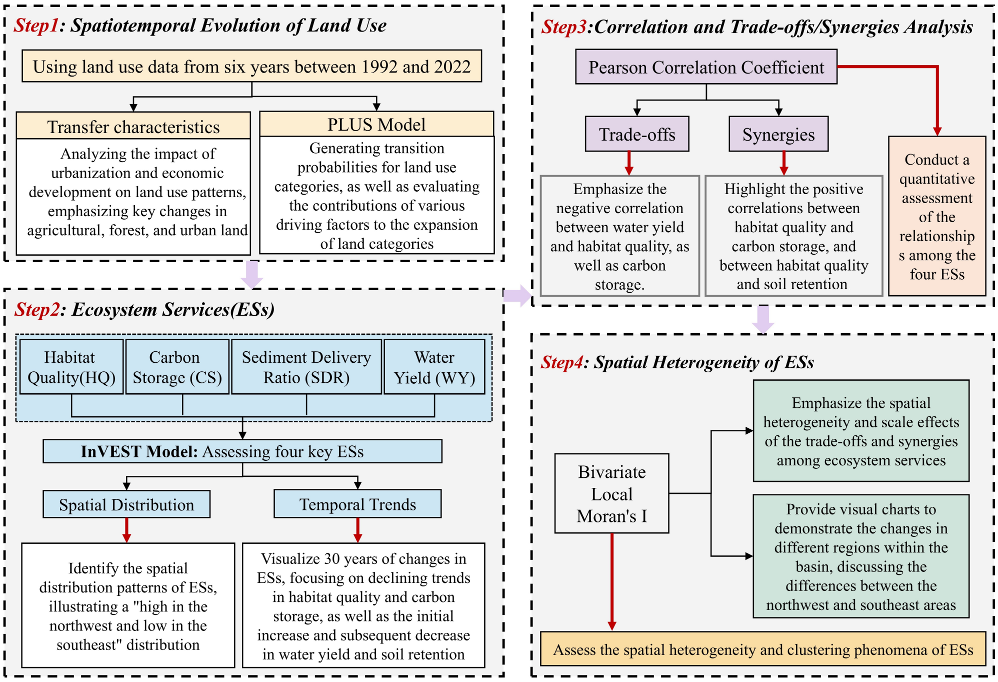

Figure 2. Research framework.

2.3.1. Land Use Transfer Matrix

The land use transfer matrix is used to quantify the patterns of LUT and their change rates over different time periods, revealing the spatiotemporal dynamics of land use. In this study, ArcGIS spatial analysis tools were employed to construct the land use transfer matrix and analyze the trends in land use conversion across different time periods. The calculation formula is as follows [16].

$$A_{ij} = \begin{bmatrix} A_{11} & A_{12} & \cdots & A_{1n} \\ A_{21} & A_{22} & \cdots & A_{2n} \\ \cdots & \cdots & \cdots & \cdots \\ A_{n1} & A_{n2} & \cdots & A_{nn} \end{bmatrix} \quad (1)$$

A_{ij} denotes the area of land type i transitioning to land type j. The i-th row corresponds to the outflow from land type i, while the j-th column indicates the destination source, representing the inflow to land type j.

2.3.2. PLUS Model

The Patch-generating Land Use Simulation (PLUS) model integrates the Land Expansion Analysis Strategy (LEAS) module to assess the spatiotemporal dynamics of LUCCs and simulate the potential for future land use expansion [17]. The LEAS module generates suitability surfaces for LUT transitions using historical data and various driving factors, representing the probability of transitions on a scale from 1 to 255. The input data includes topographic factors (elevation, slope, aspect), socio-economic indicators (GDP, population, nighttime light index), and environmental variables (average annual precipitation, soil types, vegetation types, NDVI, distance to roads, distance to water systems). The data were standardized and adjusted to a consistent spatial resolution to meet the model's requirements. The expansion probability map generated by the LEAS module was validated through visual analysis and found to be consistent with known urbanization and land expansion trends, providing references for land management policies.

2.3.3. InVEST Model

Habitat Quality (HQ)

The HQ module of the InVEST model is commonly used to assess an ecosystem's ability to support species habitats. This module calculates the HQ index, reflecting the impact of different LUTs and management scenarios on HQ. The formula is as follows [18,19].

$$Q_{xj} = H_j \left[1 - \left(\frac{D_{xj}^z}{D_{xj}^z + K^z} \right) \right] \tag{2}$$

Q_{xj} represents the HQ index 0f grid cell x; H_j is the habitat suitability for the land use type, ranging from 0 to 1; Z is the scaling constant, typically set at 2.5; K is the half-saturation constant, which is 0.5 in this study; D_{xj} denotes the habitat degradation index, indicating the extent of habitat degradation under stress conditions.

Based on previous research and the InVEST model user guide, and in combination with the actual conditions of the study area, a habitat threat factor and threat level evaluation table was constructed (Table 2), as well as a sensitivity evaluation table for LUTs to threat factors (Table 3) [20–22].

Table 2. Threat factors and threat levels.

Threat Factors	Farthest Threat Distance	Threat Degree	Declining Type
Cropland	4	0.4	Linear
Impervious	8	0.8	Exponential
Railways	7	0.7	Exponential
Barren	5	0.5	Exponential

Table 3. Sensitivity to threat factors.

LUTs	Habitat Suitability	Cropland	Impervious	Barren
Cropland	0.3	0	0.8	0.4
Forest	0.9	0.7	0.8	0.3
Grassland	0.9	0.5	0.7	0.6
Water	0.8	0.4	0.7	0.4
Impervious	0	0	0	0
Barren	0.4	0.4	0.6	0

Carbon Storage (CS)

CS is a key indicator of an ecosystem's carbon sequestration and storage capacity, reflecting its role in mitigating global climate change. This module reveals the potential impact of LUCCs and management measures on CS. The formula is as follows [23].

$$C_{total} = C_{above} + C_{below} + C_{soil} + C_{dead} \tag{3}$$

C_{total} represents the total CS (Mg/ha); C_{above} is the CS in aboveground biomass; C_{below} is the CS in belowground biomass; C_{soil} is the CS in soil; C_{dead} is the CS in dead organic matter.

This study constructed a carbon pool density table (Table 4) in consideration of the actual conditions of the study area [24,25].

Table 4. Carbon pool density (Mg/ha).

LUTs	C_Above	C_Below	C_Soil	C_Dead
Cropland	4.85	0.92	58.2	2.84
Forest	20.92	7.53	67.3	54.2
Grassland	1.63	8.48	60.2	2.19
Water	0	0	62.1	0
Impervious	0	0	60	0
Barren	0	0	53.3	0

Sediment Delivery Ratio (SDR)

SDR is a key indicator in evaluating ESs, mainly measuring the ecosystem's function in preventing soil erosion and maintaining soil quality. The application of this module helps analyze the ecosystem's contribution to maintaining soil health and reducing water and soil loss under different land management scenarios. The formula is as follows [26].

$$RKLS = R \times K \times LS \tag{4}$$

$$USLE = R \times K \times LS \times P \times C \tag{5}$$

$$SDR = RKLS - USLE \tag{6}$$

$RKLS$ indicates potential soil erosion, $USLE$ indicates actual soil erosion, and SDR indicates SDR; R represents the rainfall erosion factor, K indicates the soil erodibility factor, LS denotes the slope length factor, P indicates the soil and water conservation measures factor, and C indicates the vegetation cover and management factor.

Based on previous studies, ecological literature, and standard parameters from the InVEST model, this research constructed vegetation cover factor C and soil conservation factor P parameters (Table 5) [27] for the Qin-Mang River Basin.

Table 5. Vegetation coverage factor (C) and soil conservation measure factor (P).

LUTs	usle_c	usle_p
Cropland	0.06	0.4
Forest	0.04	1
Grassland	0.06	1
Water	0	0
Impervious	0	0
Barren	1	1

Water Yield (WY)

WY is an important indicator for assessing the water supply capacity of a region. The WY evaluation comprehensively considers factors such as average annual precipitation, potential evapotranspiration, effective vegetation water content, and soil depth, reflecting the region's water input, storage, and release processes. The assessment of WY helps researchers to understand the impact of LUCCs on water resources. The calculation formula is as follows [28].

$$Y(x) = (P(x) - AET(x)) \cdot \frac{1}{A} \tag{7}$$

$$AET(x) = P(x) \cdot \frac{PET(x)}{PET(x) + P(x)PET(x)} \tag{8}$$

$Y(x)$ is the average annual WY for cell x; $P(x)$ is the annual precipitation for cell x; $AET(x)$ is the annual actual evapotranspiration for cell x; A is the watershed area used to convert water quantity units to volume; and $PET(x)$ is the potential evapotranspiration for cell x; all units are in mm.

Based on previous research, the ecological literature, and standard parameters from the InVEST model, this study constructed biophysical parameters for each LUT (Table 6) [29].

Table 6. Biophysical parameters for various LUTs.

LUTs	Root_Depth	Kc	LULC_Veg
Cropland	2000	0.68	1
Forest	7000	0.95	1
Grassland	1700	0.62	1
Water	100	1	0
Impervious	300	0.2	0
Barren	100	0.2	0

2.3.4. Trade-Off and Synergy (TOS) Effect Analysis

The TOS effects of ESs refer to the relationships of mutual influence between different services. The trade-off effect is characterized by an increase in one ES accompanied by a decrease in another, such as agricultural expansion potentially leading to a decline in habitat quality. In contrast, the synergy effect refers to the simultaneous increase or decrease in two or more ESs, such as forest vegetation restoration, which can simultaneously enhance CS and improve soil and water conservation [30]. This study explores the TOS effects between ESs through Pearson correlation analysis and BLI analysis.

Pearson Correlation Analysis

Pearson correlation is a widely used statistical method for quantitatively assessing the linear relationship between two variables. The correlation coefficient ranges from −1 to 1, with a value of 1 indicating a perfect positive correlation, −1 indicating a perfect negative correlation, and 0 indicating no correlation. Specifically, a larger positive correlation value suggests the potential for a synergy effect between ESs, while a negative value indicates the possibility of a trade-off effect. All correlation analyses were conducted using Origin software, with the formula as follows [31].

$$r = \frac{\sum_{i=1}^{n}(x_i - \overline{x})(y_i - \overline{y})}{\sqrt{\sum_{i=1}^{n}(x_i - \overline{x})^2} \cdot \sqrt{\sum_{i=1}^{n}(y_i - \overline{y})^2}} \quad (9)$$

r is the Pearson correlation coefficient; x_i and y_i are the $i - th$ data points of the two variables; $\overline{x}$, $\overline{y}$ are the means of the two variables; and n is the sample size.

Bivariate Local Moran's I (BLI)

To further investigate the spatial distribution and interactions of ESs, this study employed BLI to explore spatial autocorrelation and clustering effects. Positive values in the Moran scatter plot indicate the presence of synergy effects between services, suggesting that they tend to increase or decrease together. Negative values, on the other hand, indicate trade-off effects, where the enhancement of one service is associated with the decline of another. The clustering map further reveals spatial aggregation effects and heterogeneity patterns. All calculations were performed using GeoDa software, with the formula as follows [32].

$$I_i = \frac{n(x_i - \overline{x}) \sum_{j=1}^{n} W_{ij}(x_j - \overline{x})}{\sum_{i=1}^{n} (x_i - \overline{x})^2} \quad (10)$$

I_i is the BLI index, n is the total number of spatial units, x_i and x_j represent the ESs quantities of regions i and j, $\overline{x}$ is the mean of the observed values, and ω_{ij} is the spatial weight.

3. Results and Analysis

3.1. Spatiotemporal Evolution of Land Use/Land Cover Change (LUCC)

LUCC in the Qin-Mang River Basin has significantly impacted the region's ESs over the past 30 years, particularly in terms of HQ and CS. This study analyzed LUT distribution maps from six time periods between 1992 and 2022 (Figure 3) using ArcGIS, revealing the spatiotemporal patterns of LUCC. The results indicate that the dominant LUTs in the basin are cropland and forestland, which together account for over 74% of the total area, while built-up land occupies approximately 10%. Notably, the expansion of built-up land is a significant trend, mainly encroaching upon cropland and forestland, while changes in water bodies are minimal. These changes reflect the profound impact of rapid urbanization and economic growth on the land use pattern of the basin, especially the ecological effects resulting from the expansion of built-up land.

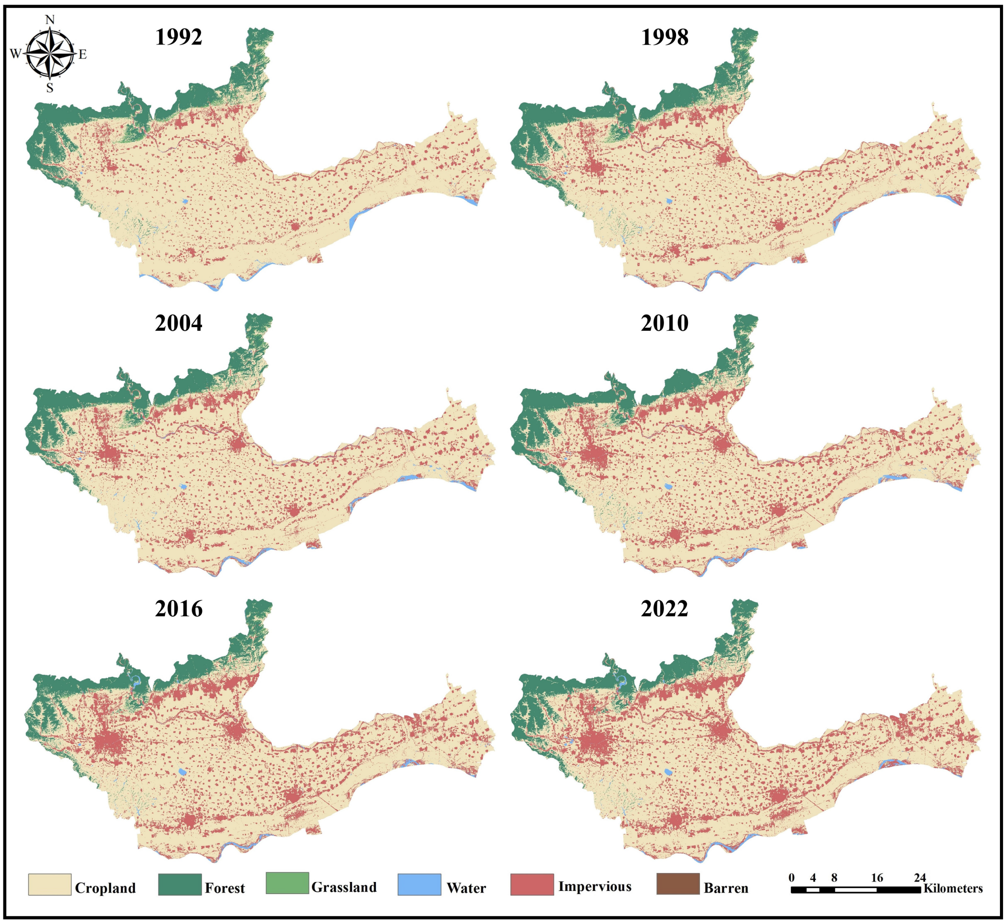

Figure 3. Distribution map of LUTs in the study area from 1992 to 2022.

Corresponding to the spatial distribution changes in land use, the temporal evolution of land use patterns also reveals spatial restructuring during the urbanization process. The study shows that the expansion of built-up land is primarily concentrated in the north-eastern and western regions of the basin. This pattern indicates that, with the acceleration of economic growth and urbanization, these areas have transitioned from agricultural land to urban land. The conversion of cropland and forestland has not only altered the land use structure but has also had a profound impact on regional ESs, particularly in terms of HQ and CS, reflecting the immense pressure that urbanization exerts on the ecological environment.

Further analysis of the land use transfer matrix (Table 7) and Figure 4 reveal the processes of LUT transitions between 1992 and 2022. Specifically, cropland decreased by 35,000 ha, mainly being converted into built-up land, reflecting the dominant role of economic development as a driving force behind LUCC. The loss of cropland resources poses a potential threat to food security and reduces its function as a carbon sink. Forestland area decreased by approximately 244.62 ha, particularly in the central and western regions, leading to a significant decline in biodiversity and ecological functions, especially in terms of forest ESs and species habitats. The Sankey diagram (Figure 5) clearly illustrates the conversion trends of different LUTs through the width and direction of the flow, providing a visual representation of the macro dynamics of LUCC.

Table 7. Land use transfer matrix for the study area from 1992 to 2022 (ha).

1992	2022							
	Cropland	**Forest**	**Grassland**	**Water**	**Impervious**	**Barren**	**Total**	**Transfer Out**
Cropland	195,899.40	1633.59	115.47	1238.85	34,946.28	4.77	233,838.36	37,938.96
Forest	5282.46	30,815.46	64.98	14.67	244.62	0	36,422.19	5606.73
Grassland	1859.31	320.76	173.52	14.58	201.06	0	2569.23	2395.71
Water	1008.72	12.96	3.78	832.77	808.83	0.09	2667.15	1834.38
Impervious	240.12	0.18	2.70	260.82	29,670.93	0.18	30,174.93	504.00
Barren	0	0	0	0	0.54	0	0.54	0.54
Total	204,290.01	32,782.95	360.45	2361.69	65,872.26	5.04	305,672.40	/
Transfer In	8390.61	1967.49	186.93	1528.92	36,201.33	5.04	/	/

Figure 6 displays the probability of future development for different land types, based on predictions generated by the PLUS model and spatial analysis with ArcGIS, revealing the trends in the expansion of different LUTs. The results show that, in the context of rapid urbanization and economic growth, the probability of expansion of built-up land is high, demonstrating the strong influence of the urbanization process on land use patterns. In contrast, the probability of expansion of cropland and forestland is declining, indicating that these natural land types will continue to face pressure from urbanization. Particularly in areas of rapid economic development, the compression of cropland and forestland will further intensify the impact on ecosystem service functions.

Figure 7a–c further illustrates the contributions of different regional characteristics to the driving factors of newly developed land types. As shown in Figure 7a, in regions with higher GDPs, the expansion of built-up land is most prominent, reflecting the strong driving effect of economic development on land expansion. Figure 7b shows that, in flat terrain areas, cropland expansion is most significant, while regions with steeper slopes face land use bottlenecks due to topographic limitations. Figure 7c reveals that, in areas with higher NDVI, forestland expansion is trending, reflecting the positive land restoration trends in regions with better vegetation coverage, influenced by ecological restoration and environmental protection measures. Overall, the economic, topographic, and ecological characteristics of different regions interact to shape the spatial patterns of LUT transformation.

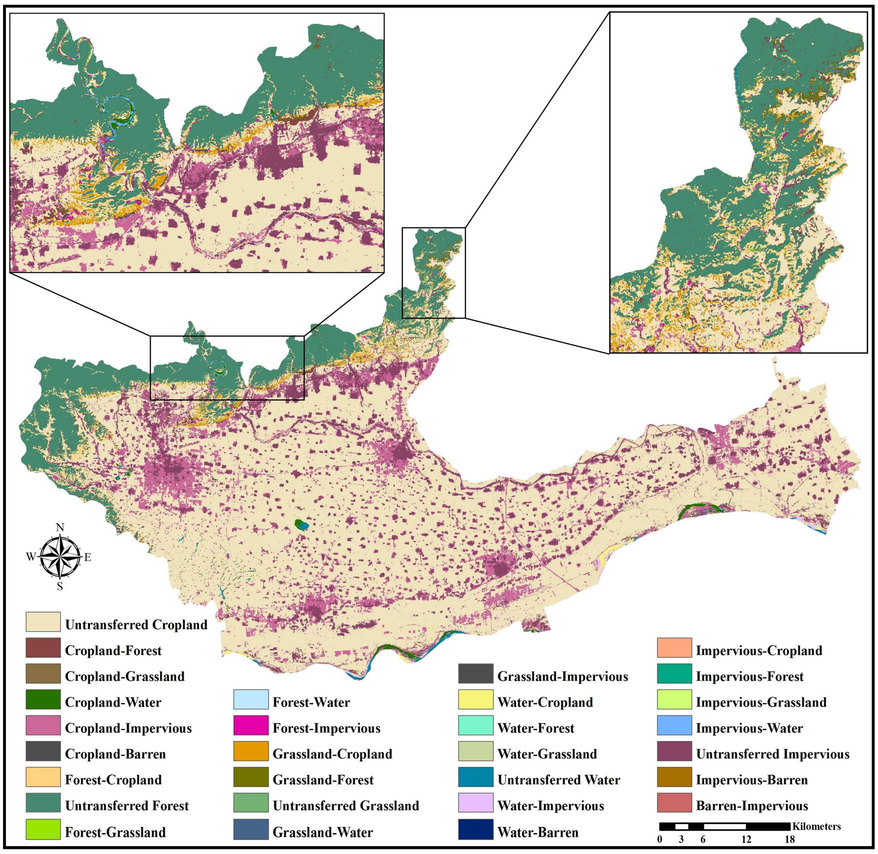

Figure 4. LUTs from 1992 to 2022.

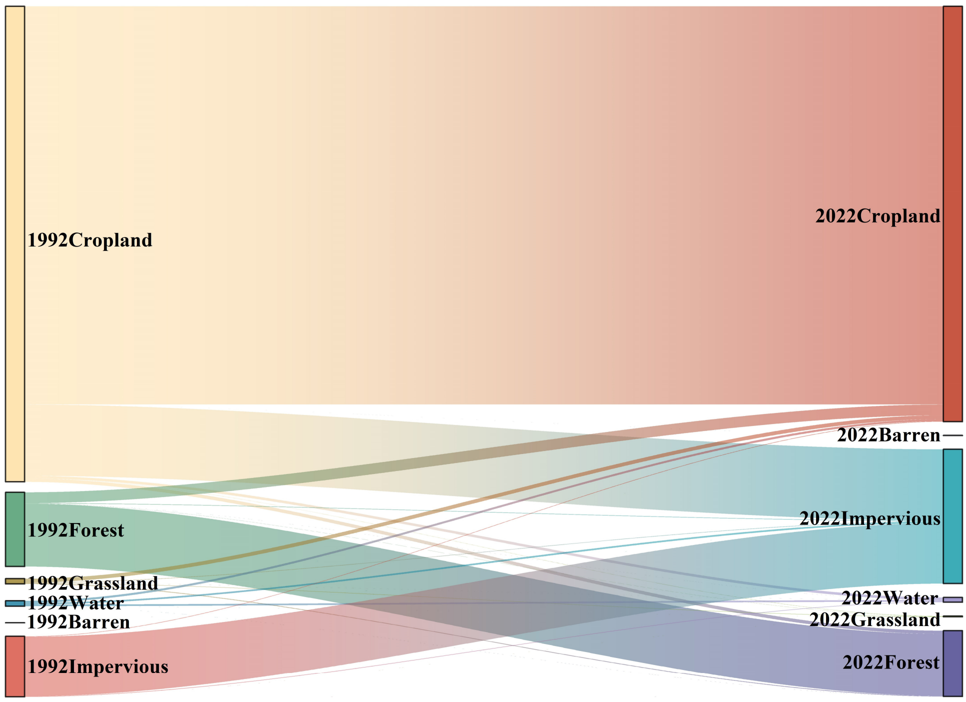

Figure 5. Sankey diagram of LUTs from 1992 to 2022.

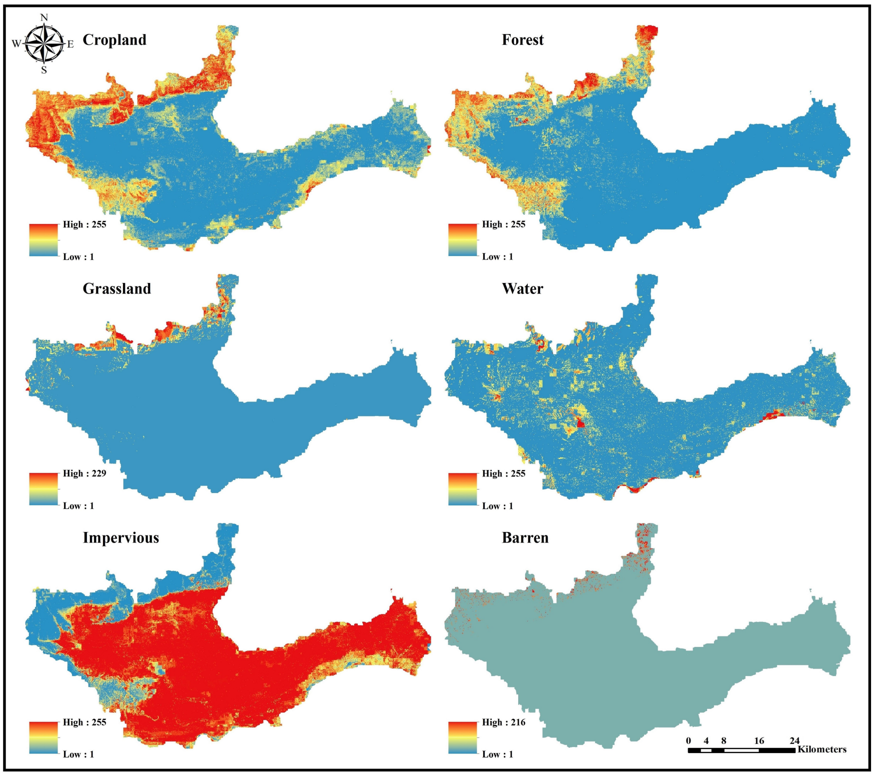

Figure 6. Development probabilities of various LUTs.

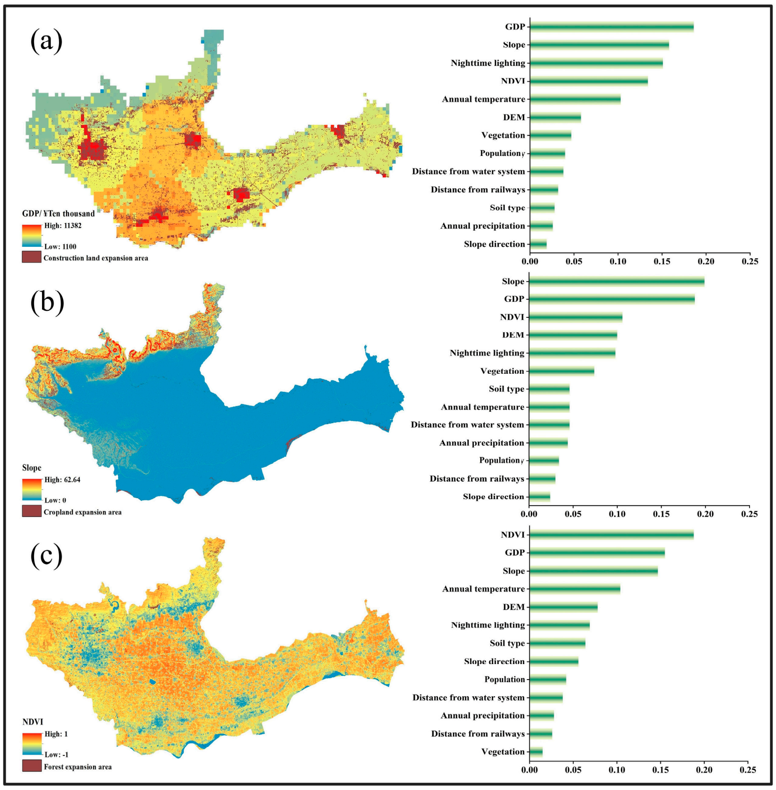

Figure 7. (**a**) Relationship between newly added built-up land and GDP level, along with the contribution of expansion driving factors; (**b**) relationship between newly added arable land and slope, along with the contribution of expansion driving factors; (**c**) relationship between newly added forest land and NDVI values, along with the contribution of expansion-driving factors.

3.2. Spatiotemporal Evolution of Ecosystem Services (ESs)

3.2.1. Spatiotemporal Evolution of Habitat Quality (HQ)

Based on the InVEST model, the evaluation of HQ in the Qin-Mang River Basin from 1992 to 2022 (Figure 8) indicates a persistent decline in HQ across the basin. The HQ index decreased from 0.34 in 1992 to 0.29 in 2022, with the spatial variation in HQ increasing, as reflected by the rise in standard deviation from 0.16 to 0.19. This change reflects the overall degradation of the ecological environment, particularly in the southern and eastern regions where HQ deterioration is more pronounced. Figure 8 clearly illustrates this trend, with some mountainous areas and nature reserves maintaining relatively good HQ, but with the majority of regions, especially those experiencing rapid urbanization, showing significant declines in HQ.

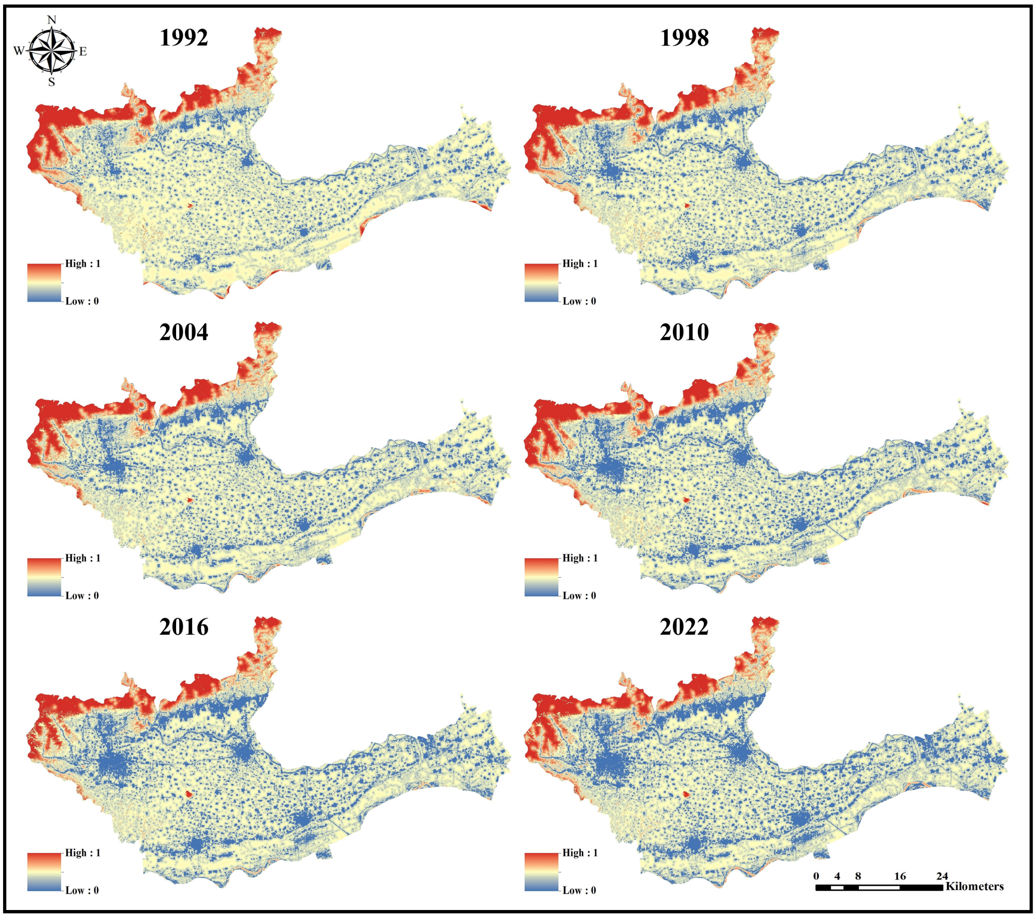

Figure 8. Temporal and spatial distribution map of HQ index.

The primary cause of this decline is closely linked to the accelerated urbanization process and the expansion of built-up land. Specifically, urbanization has intensified human interference with natural ecosystems, leading to the disruption of habitat continuity and integrity, especially in ecologically fragile areas where degradation has significantly accelerated. Additionally, LUCCs, particularly the conversion of agricultural and forested lands, have further exacerbated the degradation of HQ. The relationship between the reduction in agricultural land and the expansion of urban areas in the basin reflects the direct impact of human activities on ecosystem health.

3.2.2. Spatiotemporal Evolution of Carbon Storage (CS)

From 1992 to 2022, CS in the Qin-Mang River Basin exhibited significant spatial variation (Figure 9). Overall, CS follows a “high in the northwest, low in the southeast” distribution pattern. The northern and northwestern regions have higher CS, primarily due to the good ecological conditions of the western Henan mountains and the Taihang Mountains, coupled with higher vegetation coverage. In contrast, the southeastern region, characterized by extensive built-up areas and water bodies, has lower CS, weaker vegetation coverage, and a reduced carbon sequestration capacity. This spatial distribution difference is closely related to both the natural conditions and the spatial distribution of human activities in the basin.

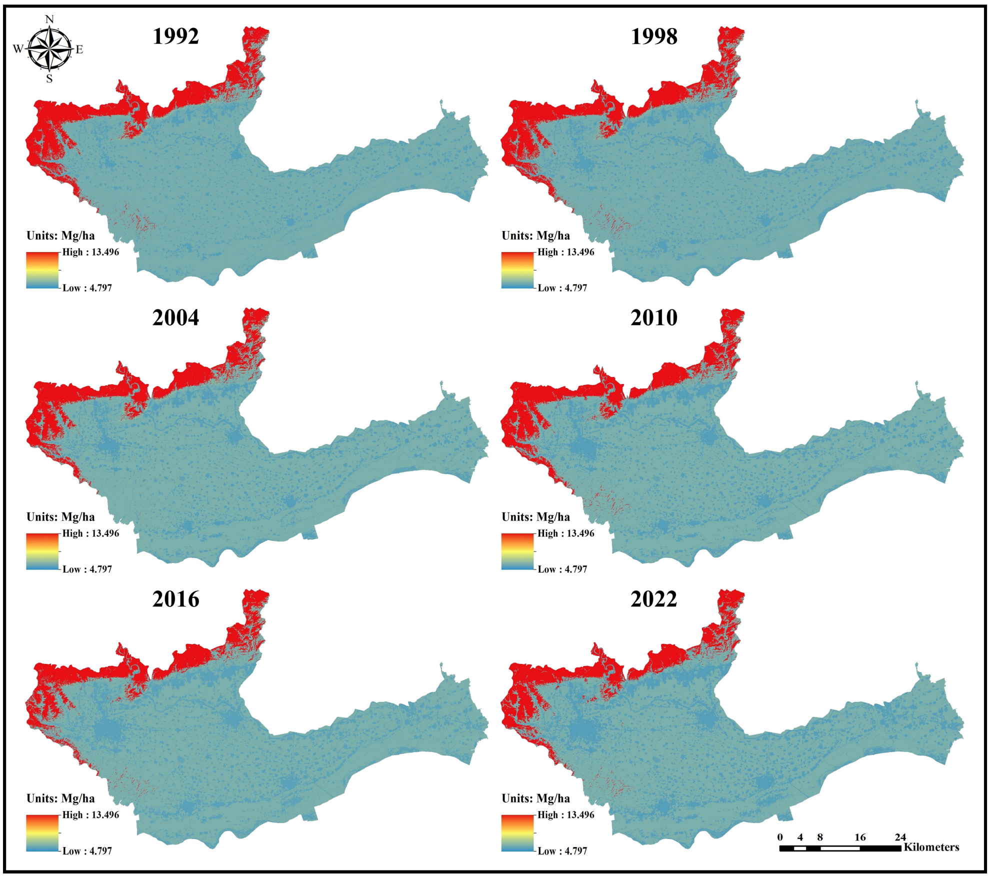

Figure 9. Temporal and spatial distribution map of CS.

Time-series analysis shows that, while the CS in high-carbon areas remained stable, the extent of low-carbon areas gradually expanded, particularly in regions with accelerating urbanization. The trend in Figure 9 indicates that urban expansion has led to significant LUCCs, particularly the continuous increase in built-up land, resulting in a reduction in CS in some areas. Notably, in the central and southern regions, as built-up land expanded, areas originally rich in CS were gradually transformed into low-carbon areas. This phenomenon suggests that rapid urbanization not only altered land use patterns but also impacted the spatial distribution of regional CS and ecological functions.

3.2.3. Spatiotemporal Evolution of Sediment Delivery Ratio (SDR)

SDR in the Qin-Mang River Basin exhibited significant spatial variability between 1992 and 2022 (Figure 10). Overall, the distribution follows a "high in the northwest, low in the southeast" pattern. The southern section of the Taihang Mountains in the north, with good vegetation and significant topographical variation, became a high-value zone for SDR. In contrast, the southeastern plains, with a high degree of land development, exhibited weaker SDR. The changes in SDR reflect the influence of different topographies and land use practices on soil conservation functions.

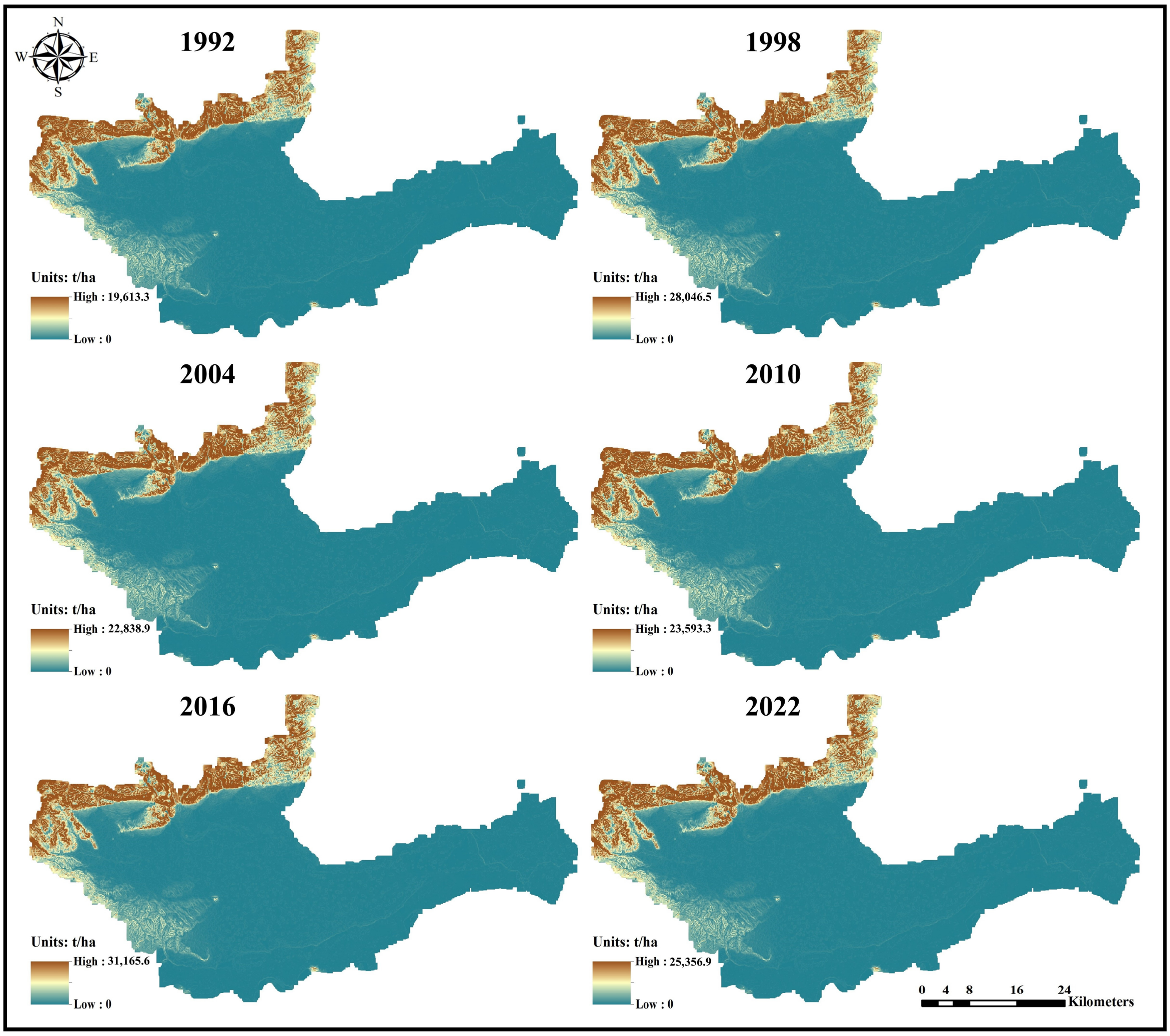

Figure 10. Temporal and spatial distribution map of SDR.

Time-series analysis shows that the volume of SDR initially increased and then decreased. From 1992 to 2016, the volume of SDR increased from 19,613.3 t/ha to 31,165.6 t/ha, but by 2022, it had declined to 25,356.9 t/ha. This change is closely related to LUCCs, topographical features, and vegetation cover. Particularly in the southeastern region, rapid urbanization, the reduction in agricultural land, and the expansion of built-up land severely impacted SDR. In contrast, the northwest region, with better vegetation protection, maintained a relatively stable level of SDR.

3.2.4. Spatiotemporal Evolution of Water Yield (WY)

The WY from 1992 to 2022 in the Qin-Mang River Basin, calculated using the InVEST model based on average annual precipitation, evapotranspiration, and root limiting layer depth data, shows a "high in the southeast, low in the northwest" distribution pattern (Figure 11). The southeastern region, with abundant precipitation and lower elevation, has a higher WY capacity, while the northwestern mountainous areas, with high evapotranspiration and low precipitation, have a lower WY capacity. Although the overall spatial distribution of WY did not change significantly, the rapid urbanization process, particularly in the central region, has negatively impacted WY services.

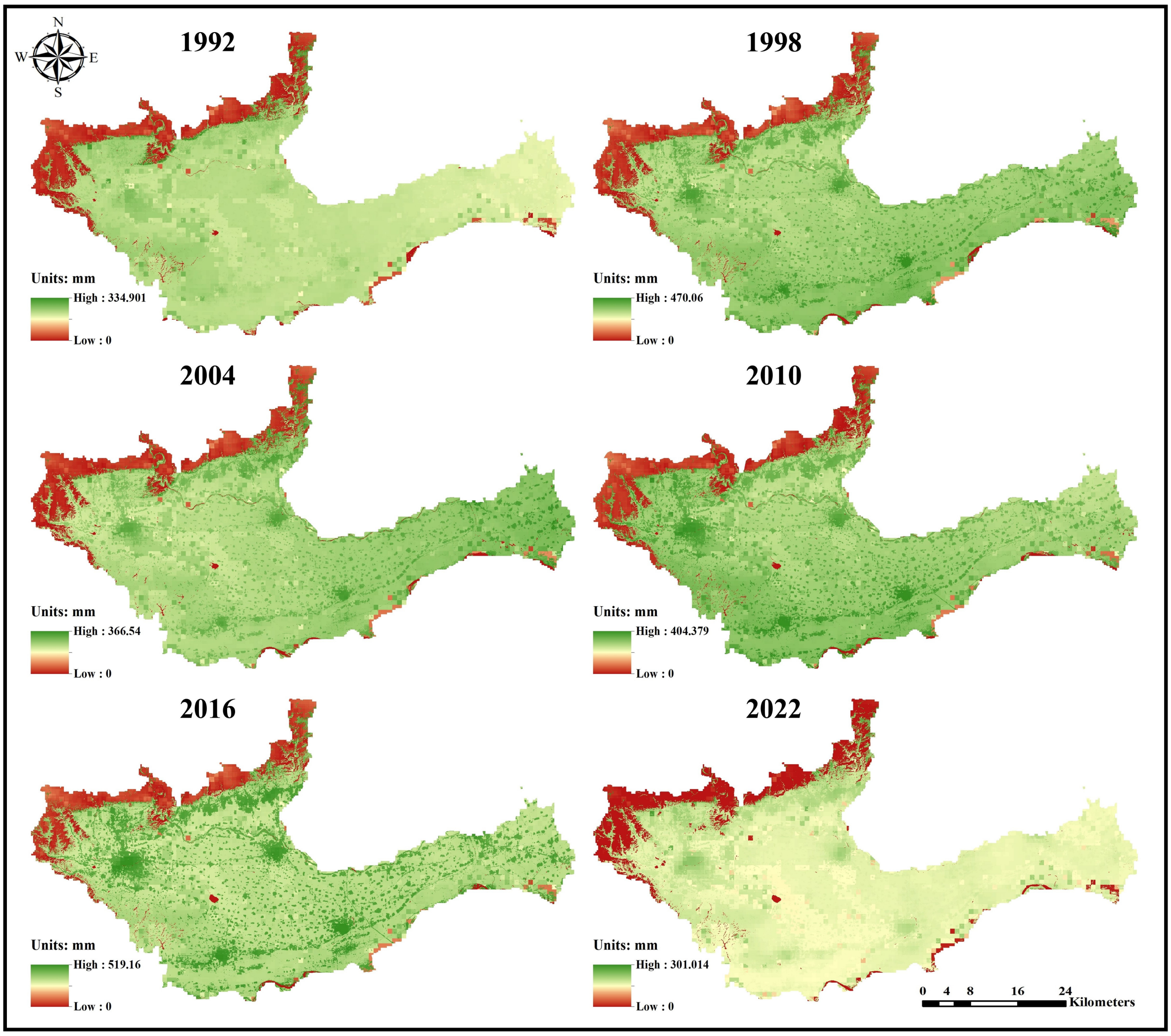

Figure 11. Temporal and spatial distribution map of WY.

Time-series analysis (Table 8) shows significant fluctuations in WY across different periods, with the highest yields recorded in 1998 at 796 million cubic meters and 831 million cubic meters in 2016, but with a sharp decline to 400.45 million cubic meters in 2022. This significant drop is closely related to changes in precipitation, increased evapotranspiration, and inadequate water resource management. Figure 11 further illustrates the spatial distribution of these changes and reveals the compressive effect of urban expansion on water resource yields, particularly in areas with reduced agricultural land, where the availability of water resources has been greatly impacted.

Table 8. ESs function quantities in the study area from 1992 to 2022.

Year	HQ	CS/10^6 t	SDR/10^8 t	WY/10^6 m³
1992	0.34	23.18	4695.05	460.39
1998	0.33	22.04	6924.59	796.06
2004	0.32	22.83	5738.28	594.28
2010	0.30	22.64	5677.55	620.46
2016	0.29	22.52	7723.19	831.17
2022	0.29	22.62	6470.34	400.45

Table 8 presents the trend in ecosystem service function changes from 1992 to 2022 in the study area. The HQ index decreased from 0.34 to 0.29, reflecting the deterioration of regional ecosystem health, which is closely linked to increasing human activities, urbanization, and LUCCs. CS remained between 22 and 23 million tons throughout the study period, with minor fluctuations, but failed to return to 1992 levels, suggesting that, while the region has some carbon sequestration capacity, its long-term low level may weaken its ability to mitigate climate change. SDR fluctuated significantly from 1992 to 2016, peaking at 69.24 million tons in 1998 and increasing to 77.23 million tons in 2016, but dropped to 64.7 million tons by 2022, reflecting the negative impact of human activities on soil quality. WY fluctuated greatly, reaching 796 million cubic meters in 1998 and 831 million cubic meters in 2016, but falling sharply to 400.45 million cubic meters in 2022, reflecting significant declines caused by changes in precipitation, increased evapotranspiration, and inadequate water resource management.

3.3. Trade-Off and Synergy (TOS) Among Ecosystem Services (ESs)

3.3.1. Correlation Analysis of TOS in ESs

The changes in the correlation between ESs in the Qin-Mang River Basin from 1992 to 2022 reveal the dynamic processes of functional TOS (Figure 12). The study indicates that, over time, the synergy between ESs gradually weakened in some years, while trade-offs became more pronounced in certain regions. Specifically, in 1992, the correlation coefficient between HQ and CS was 0.86, indicating a significant synergy; the correlation coefficient between HQ and SDR was 0.66, also suggesting a strong synergistic relationship. However, the negative correlation between HQ and WY (−0.20) indicated a potential trade-off between ESs. In 1998, the correlation coefficient between HQ and CS increased to 0.91, suggesting an enhanced synergy. However, the negative correlation between HQ and WY increased to −0.42, reflecting a clear trade-off between high HQ and low WY in some areas. In the same year, the positive correlation between CS and SDR was 0.75, while the negative correlation between CS and WY was −0.52, further illustrating the competition between WY and CS.

By 2004, the correlation coefficient between HQ and CS remained at 0.91, continuing to show a strong synergy. However, the negative correlation between HQ and WY (−0.40) began to strengthen. This trend indicates that, although the synergy between CS and HQ persisted, the negative trade-offs between WY and other ESs were intensifying. In 2010 and 2016, the correlation coefficient between HQ and CS remained stable at 0.91, and the synergy between HQ and SDR remained strong (0.71 and 0.68), but the negative correlation between HQ and WY remained between −0.40 and −0.45, suggesting that changes in WY had a significant impact on the relationships between ESs. By 2022, the correlation coefficient between HQ and CS was 0.90, continuing to show a strong synergy. However, the negative correlation between HQ and WY increased to −0.36, indicating that the competitive relationship between ESs was more pronounced in certain regions. The positive correlation between CS and SDR (0.73) and the negative correlation between CS and WY (−0.41) continued to reflect the trade-offs between WY and other ESs.

Overall, as urbanization progresses and LUCCs increase in the Qin-Mang River Basin, the synergy between ESs has gradually weakened, while trade-offs have become more significant in certain areas. Specifically, between HQ, CS, SDR, and WY, the competitive relationships between ESs have increasingly intensified over time, especially in areas with WY stress. This change not only reveals the mutual constraints between ecosystem service functions but also reflects the profound impact of LUCCs on ESs. To address this challenge, it is urgent to optimize land use patterns, control urbanization, and promote sustainable land management strategies to enhance positive synergies between ESs and mitigate negative trade-offs.

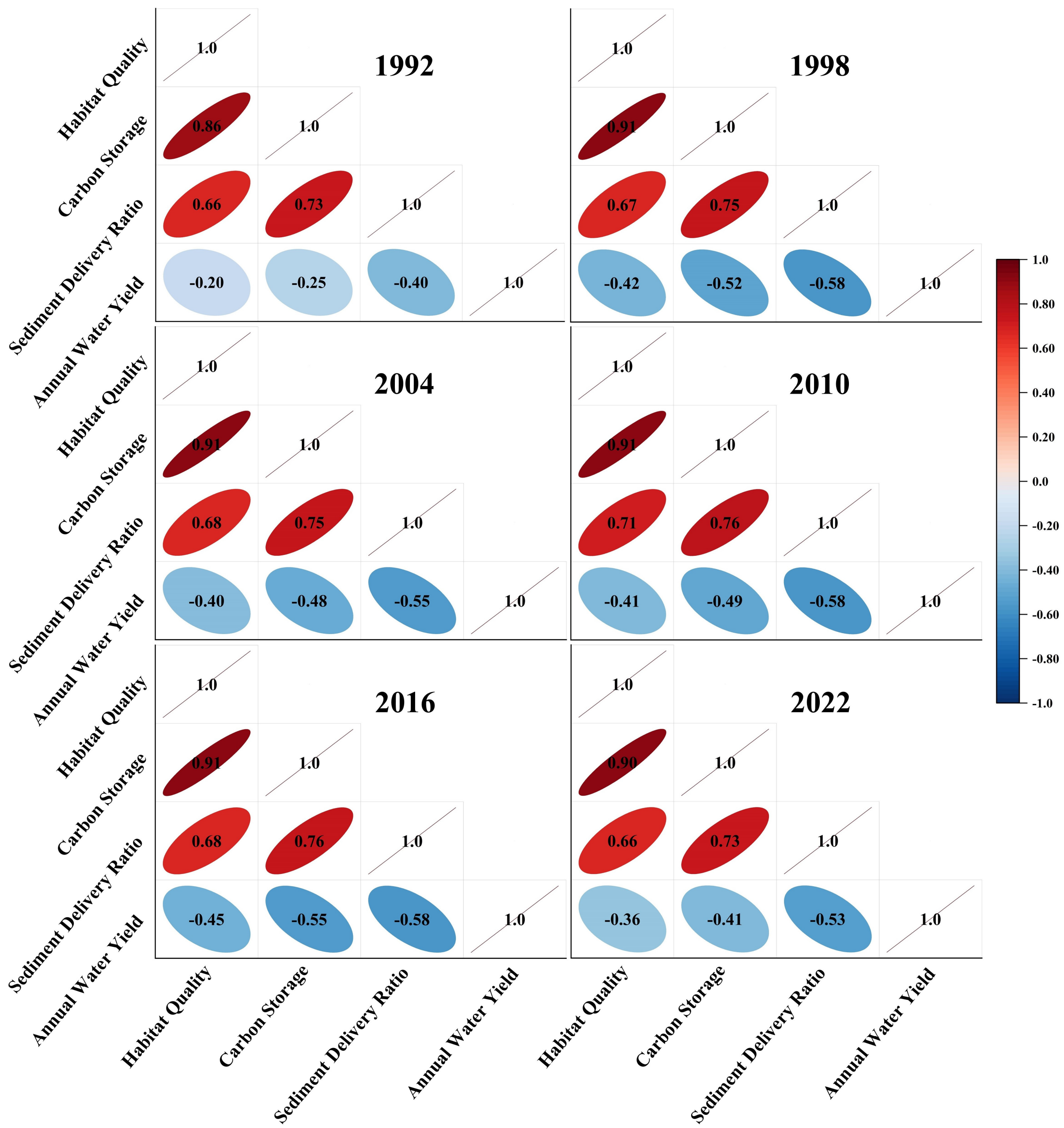

Figure 12. Correlation analysis of four ESs in the study area from 1992 to 2022.

3.3.2. Spatial Distribution and Heterogeneity of TOSs in ESs

Figure 13 presents the BLI clustering map of ESs in the Qin-Mang River Basin in 1992, while Figure 14 further reveals the spatial relationships between ESs through scatter plots. The results indicate that there is a significant positive spatial autocorrelation between HQ and CS (Moran's I = 0.713), HQ and SDR (Moran's I = 0.630), and CS and SDR (Moran's I = 0.702), while there is a significant negative spatial autocorrelation between HQ and WY (Moran's I = −0.331), CS and WY (Moran's I = −0.407), and SDR and WY (Moran's I = −0.514). All Moran's I values passed the significance test (P values were all less than 0.05), and, through randomization tests, the probability of these clustering patterns being generated was less than 1%, indicating the statistical significance of these spatial autocorrelation relationships.

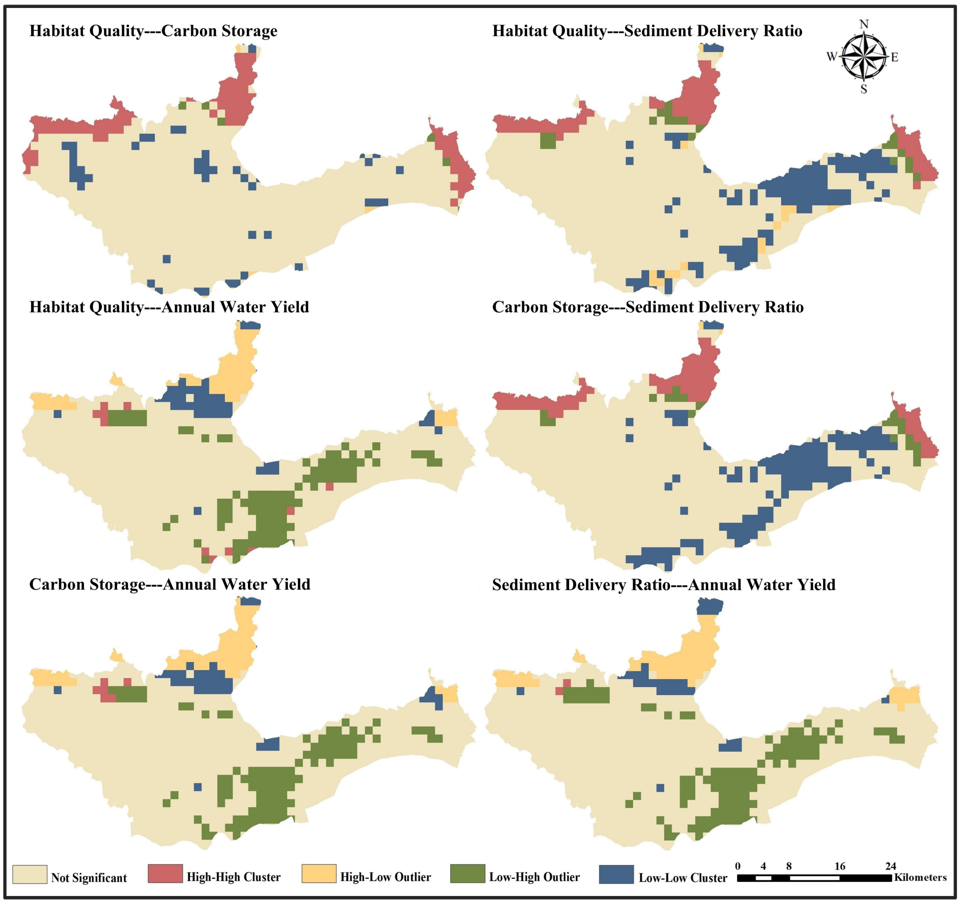

Figure 13. Spatial distribution map of TOSs among ESs in 1992.

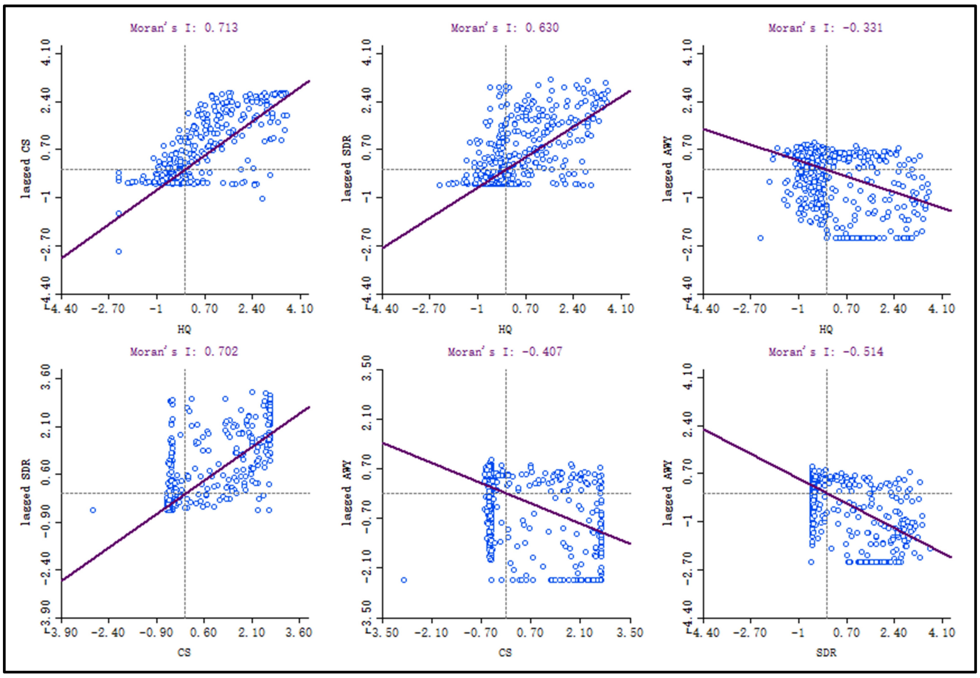

Figure 14. BLI scatter plot for 1992.

The spatial analysis in 1992 showed that in the northern and northwestern parts of the study area, HQ, CS, and SDR exhibited significant positive spatial autocorrelation, forming high-value clusters of ecosystem service functions. The strong positive spatial autocorrelation indicates significant synergies between ESs in these regions, particularly the high correlations between HQ and CS and CS and SDR. This phenomenon reflects the relatively favorable ecological conditions in these areas, such as good vegetation coverage and minimal ecological disturbance, which promote the mutual enhancement and coordinated development of ESs. However, there was a significant negative spatial autocorrelation between WY and HQ, CS, and SDR, indicating that, in some regions, higher ecological service functions (e.g., HQ, CS, and SDR) were accompanied by lower WY. This negative correlation reveals the spatial heterogeneity of ecosystem service functions, particularly in areas with low WY, where high-value ecological functions such as HQ and CS tend to concentrate in spatial units corresponding to lower WY.

The BLI clustering map further confirmed this spatial aggregation phenomenon. The high-value regions in the study area were mainly concentrated in the northern mountainous areas, while low-value regions were primarily distributed in the southeast. This spatial pattern highlights the significant spatial heterogeneity of ecosystem service functions, particularly the contrast between high-value and low-value areas. Specifically, the ecosystem service functions in the northern mountainous areas were stronger, reflecting the stability of the natural ecological environment and the synergies between ESs in these areas. In contrast, the southeastern region exhibited weaker ecosystem service functions due to factors such as the expansion of construction land and a decline in vegetation coverage, leading to a significant reduction in the synergies between services.

By 2022, the spatial distribution of ESs in the Qin-Mang River Basin had undergone significant changes (Figure 15). Particularly in the southern and eastern regions, the trade-off phenomena between ESs became more pronounced, with the negative correlations between HQ and WY and between SDR and WY strengthening in these areas. The spatial autocorrelation analysis in 2022 revealed an increase in the number of low-value regions, where ESs experienced severe degradation, the synergies between services were significantly weakened, and trade-off phenomena were significantly exacerbated. The BLI scatter plot showed (Figure 16) that there was a significant positive spatial autocorrelation between HQ and CS (Moran's I = 0.731), HQ and SDR (Moran's I = 0.643), and CS and SDR (Moran's I = 0.706), while significant negative spatial autocorrelation was found between HQ and WY (Moran's I = −0.366), CS and WY (Moran's I = −0.405), and SDR and WY (Moran's I = −0.527). All results had P values less than 0.05, and, through randomization tests, the probability of these clustering patterns being generated was less than 1%, confirming the statistical significance of these spatial autocorrelation relationships.

In the spatial analysis of 2022, the spatial aggregation effect of low-value regions was particularly prominent, reflecting the significant negative impact on ecosystem service functions in these areas. This change is closely related to the accelerating urbanization process, the expansion of construction land, and unsustainable land use patterns. Specifically, with the acceleration of urbanization, the land cover types in the southern and eastern regions have undergone significant changes, and the expansion of construction land and ecological degradation have intensified the competition and conflicts between ESs.

This negative spatial aggregation effect poses a major challenge to the synergies of ESs. In particular, the negative correlations between WY and HQ, CS, and SDR reveal the mutual constraints between ESs in these regions. As ecological degradation intensifies, the ecosystem functions in these areas further deteriorate, leading to the formation of distinct low-value regions in the spatial distribution of ESs. This trend poses a severe challenge to regional ecological stability and sustainable development.

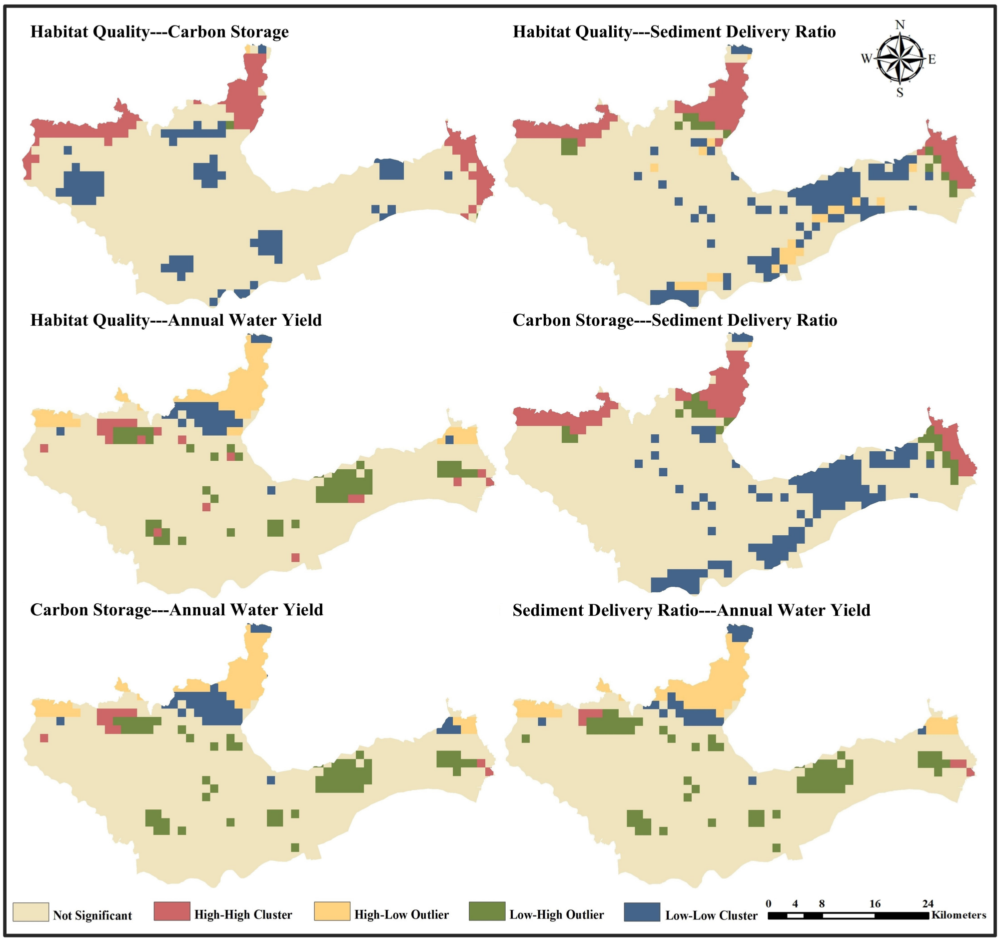

Figure 15. Spatial distribution map of TOSs among ESs in 2022.

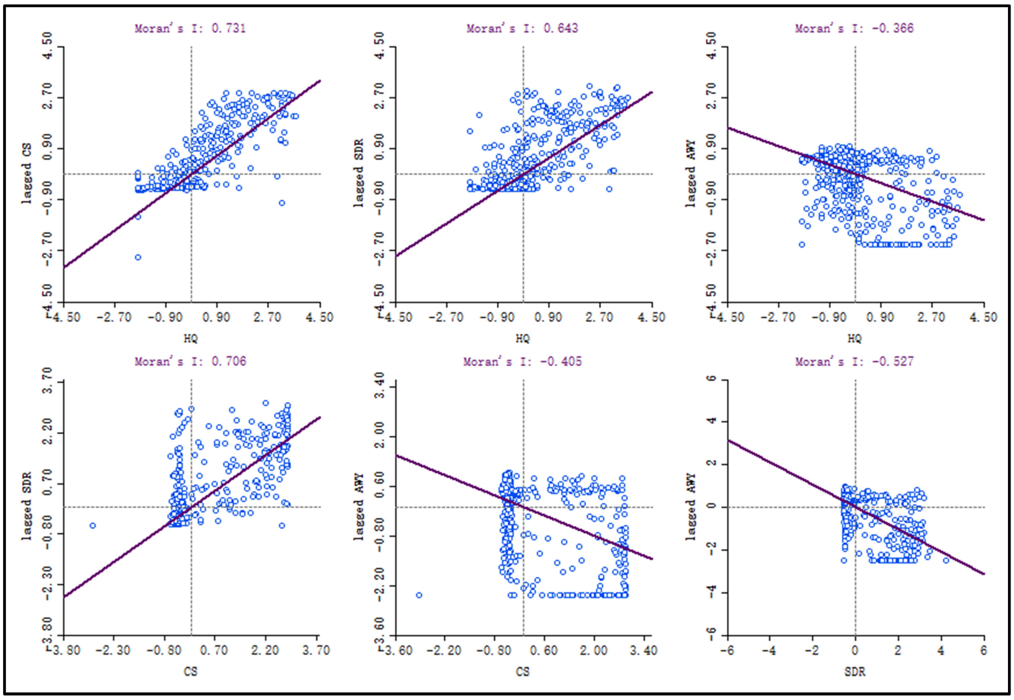

Figure 16. BLI scatter plot for 2022.

4. Discussion

4.1. Interpretation and Comparison of Results

This study demonstrates that LUT transformation in the Qin-Mang River Basin over the past 30 years has been driven by urbanization and economic development, leading to significant changes in the land use pattern of the basin. Although LUCC has stabilized in recent years, the expansion of construction land remains the main trend, which is primarily achieved through the reduction in cultivated land and forest areas. This trend highlights the profound impact of urbanization on the ecological environment, resulting in the weakening of critical ESs.

The expansion of construction land encroaching on cultivated land and forests indicates a close relationship between urbanization and LUT transformation. These transformations have significantly impaired the region's ecosystem service capacity, particularly in terms of HQ, CS, and SDR. The decline in HQ is directly related to the conversion of natural land types to urban areas, and this finding is consistent with research conducted in other urbanized regions [33,34]. This study further confirms the negative impact of urbanization on ecosystem functions, particularly in other regions of the Yellow River Basin, where trends of habitat degradation and decreased CS have also been validated [35]. These studies suggest that urbanization not only leads to the loss of natural habitats but also exacerbates habitat fragmentation, which further affects biodiversity and ecosystem resilience [36].

In terms of spatial distribution, this study found significant regional differences in ESs within the basin, particularly in the northwest and southeast. The northwest region has stronger ecological service functions, while the southeast region is more vulnerable. This disparity suggests that future land management and conservation policies should consider local differences and develop specific strategies [37]. For example, ecological protection measures should be prioritized in the high-ecological-value areas of the northwest, while ecological restoration should be strengthened in the urbanized areas of the southeast to mitigate the negative impacts of urbanization on the ecosystem.

The results of this study further emphasize that policymakers should integrate ecological restoration measures, such as forest rehabilitation and soil and water conservation, into urban planning to achieve a sustainable balance between urbanization and ecosystem integrity. Additionally, considering the importance of spatiotemporal dynamics in land use and ecosystem service management is crucial. The Qin-Mang River Basin, as a key ecological region, plays an irreplaceable role not only in biodiversity conservation but also in maintaining regional ecological stability. Therefore, regional management strategies should place a high priority on the sustainability of ESs to ensure the long-term health and stability of ecosystems.

4.2. Mechanisms of Trade-Offs and Synergies (TOSs)

This study delves into the impact of LUCCs on the TOSs between ESs. Correlation analysis reveals that there are complex interactions between Ess, such as HQ, CS, SDR, and WY, and these relationships dynamically change with shifts in land use. Specifically, there is a positive correlation between HQ and CS, indicating that healthy habitats help enhance carbon sequestration, thereby boosting ecosystem CS. This finding is consistent with studies from other regions, where large-scale ecological restoration or forest protection projects typically improve both HQ and CS [38].

However, excessive water resource development significantly affects the synergy and trade-off relationships between ESs. While water resource development may enhance WY services in the short term to support agricultural, industrial, and urban needs, long-term overexploitation leads to habitat degradation, increased soil erosion, and reduced CS, resulting in ecological degradation. When water resource development intersects with

LUCCs, it often exacerbates ecological degradation, such as the drying of water bodies and reduction in wetlands, which affects biodiversity and ecosystem restoration capacity. The negative correlation between water resource development and other ecological functions, such as HQ and WY, has been validated in studies of multiple river basins [39].

As urbanization accelerates, the synergy between ESs weakens, and trade-off relationships become more pronounced. Particularly in areas of construction land expansion and reduction in cultivated land, CS and SDR continue to decline, while WY fluctuates in some regions. This trade-off mechanism is especially evident in areas where urbanization is intensifying, highlighting the pressure urban expansion places on the multifunctionality of ESs. Similar conclusions have been found in both domestic and international studies, where rapid urbanization in the Yangtze River Basin and the Brazilian Amazon has led to negative trade-offs between ESs [40].

This study also analyzes the impact of urbanization on the synergy between WY and CS. As urbanization accelerates, the expansion of built-up areas reduces the amount of green land and forests, which in turn diminishes the capacity for water source conservation, thereby affecting WY. Simultaneously, the decrease in land permeability not only reduces groundwater recharge but also exacerbates soil erosion, further weakening SDR functions [41]. These cumulative effects lead to a gradual reduction in the synergy between water source conservation and CS, particularly in highly urbanized areas such as the southeastern part of the Qin-Mang River Basin, where a clear trade-off relationship emerges. As green land area shrinks and water source conservation zones decrease, the negative trade-off between WY and CS becomes more pronounced. This trend is commonly observed in other watersheds with similar urbanization backgrounds, indicating that the question of how to coordinate the joint enhancement of water source conservation and CS remains a key issue for future urban development.

4.3. Spatial Heterogeneity and Scale Effects

This study found that the impact of LUT transformation on ESs exhibits significant spatial heterogeneity. This variability is closely related not only to the type and intensity of land use but also to regional natural environmental conditions and socioeconomic development. The presence of spatial heterogeneity indicates that ESs show marked spatial distribution differences across regions. For example, in the northern mountainous areas of the basin, due to the higher vegetation cover, ESs such as SDR, CS, and HQ are stronger. This is closely related to the lower level of urbanization and relatively intact natural ecosystems in the region. In contrast, in the southeastern areas, urbanization has accelerated, leading to significant expansion of construction land, resulting in a marked decline in services like HQ, SDR, and CS, demonstrating weaker ecological service functions.

Spatial heterogeneity not only reflects the direct impact of different land use patterns on ESs but is also constrained by various factors such as topography, climate conditions, and population density and economic development. For instance, the northern mountainous areas, with their higher altitude and complex terrain, are more resilient to external disturbances, and their ESs remain stable. In contrast, the lowland plain areas in the southern and eastern parts of the basin, characterized by flat terrain and convenient transportation, experience higher levels of urbanization. LUCCs in these areas have more significant impacts on ESs, particularly in terms of habitat fragmentation and ecosystem degradation. This conclusion is consistent with findings from other studies, such as those in the Yangtze River region, where areas with higher urbanization levels also show significant declines in ecosystem service functions [42].

Building on this, this study further explores the impact of temporal and spatial scales on ESs. Through spatiotemporal scale analysis, it was found that the trend of ecosystem service changes is not only closely related to spatial location but is also significantly influenced by changes in the temporal scale. Over shorter time scales (e.g., within 10 years), LUCCs have a more direct impact on ESs, particularly during urbanization, where the expansion of construction land has a significant negative effect on HQ and CS. Meanwhile, over longer time scales (e.g., 30 years or more), changes in ESs show more complex dynamic characteristics, closely related to long-term LUT transformation and policy interventions.

Specifically, over the past 30 years, the HQ and CS in the Qin-Mang River Basin have shown a significant declining trend, which is not only due to intensified urbanization but also the reduction in agricultural land and the decline in forest cover. In the short term, the expansion of construction land may lead to a rapid decline in ESs. However, in the long term, ecological restoration measures (such as converting farmland to forests and wetland restoration) can mitigate the trend of ecological degradation to some extent, as seen in preliminary ecological restoration projects in the central and eastern parts of the basin.

Moreover, scale effects are also particularly pronounced in spatiotemporal scale analysis. At larger scales (regional scale), the impact of LUCCs is more pronounced, and the interrelationships between ESs are more complex. At smaller scales (such as at the local watershed level), changes in ESs are more influenced by local environmental conditions [43]. Therefore, when formulating land use planning and ecological restoration policies, it is essential to consider the influencing factors at different scales and adopt corresponding management measures.

4.4. Policy Recommendations and Practical Implications

This study provides theoretical foundations and practical guidance for land use policy and management. As urbanization progresses, the spatiotemporal variability of ESs requires policymakers to carefully consider regional differences and their impacts on ecological functions in planning. In areas with high ecological value (such as the northern mountainous regions of the basin), priority should be given to protecting natural ecosystems, restricting excessive development, and preventing the expansion of construction land as well as irrational agricultural and industrial development to ensure that ecological functions remain intact. Special emphasis should be placed on the protection of key ecological resources, such as forests, grasslands, and wetlands, to maintain regional ecosystem stability.

In the central, southern, and eastern parts of the basin, where urbanization is accelerating, ecological degradation is becoming more severe. There is an urgent need to implement strict ecological red-line protection policies to prevent further exacerbation of ecological degradation. In already degraded areas, large-scale ecological restoration measures, such as afforestation, converting farmland back to forests, and wetland restoration, should be implemented to enhance CS, water conservation capacity, and biodiversity. These efforts can be combined with ecological engineering techniques, such as the construction of ecological barriers and soil moisture management, to further improve ecological restoration outcomes.

This study emphasizes the necessity of region-specific land use policies through spatiotemporal scale analysis. Considering the regional differences in ESs, future land use policies should adopt more precise regional strategies to ensure a reasonable balance between land use and ecological protection needs in different ecological environments. For instance, in regions with higher ecological value, stricter ecological management measures should be implemented. In more urbanized areas, green infrastructure construction and ecological restoration measures should be adopted to gradually achieve a win-win situation for both ecology and economy.

Beyond existing ecological protection and restoration policies, this study also recommends the incorporation of innovative policy tools to enhance ESs. Ecological compensation mechanisms, for example, could incentivize land developers or urban planners to compensate for the loss of ecological functions, thereby assisting in the restoration of the ecological value of affected areas. Furthermore, the implementation of green infrastructure (such as urban greenbelts, ecological parks, and rooftop greening) could effectively enhance urban ecological functions and mitigate the pressures of urbanization on ecosystems. While these policy measures contribute significantly to the enhancement of ESs, local governments may face challenges such as economic constraints, limited management capacity, and public awareness. Therefore, future policy-making should emphasize interdepartmental collaboration and increased public participation to foster a shared commitment to ecological protection, helping to address the challenges posed by rapid urbanization.

4.5. Research Limitations and Future Approaches

Despite this study's in-depth exploration of the impact of LUCCs on ESs, some limitations remain. First, the land use data used in this study have relatively low resolution, which may affect the results of local scale analyses. Second, this study did not explore the impact of other factors, such as climate change, on ESs. Future research could integrate climate change considerations into the assessment framework for ESs.

Future research could focus on the following aspects: first, improving data resolution for more refined spatial analyses; second, examining the combined impacts of climate change and other stressors on ESs; and third, conducting long-term dynamic monitoring to identify long-term trends and patterns in ecosystem service changes.

5. Conclusions

This study evaluated the impact of LUT transformation on ESs in the Qin-Mang River Basin using multiple methods, revealing the spatiotemporal dynamics between LUCCs and ESs, along with the driving mechanisms behind them. The main conclusions are as follows:

(1) The LUCCs in the Qin-Mang River Basin have significantly affected ESs. In recent years, the expansion of built-up land has primarily encroached upon arable land and forests, reflecting the close relationship between urbanization and economic development. Over the past 30 years, the area of arable land has decreased by 35,000 hectares, which were converted into built-up land. This change is primarily driven by economic development, posing significant threats to food security and ecosystem service functions. The LUT transition matrix analysis further reveals that the probability of future expansion of built-up land is relatively high, while the probability of expansion for arable land and forests is relatively low, reflecting the immense pressure of urbanization on natural land.

(2) LUCCs have significantly affected ESs, exhibiting certain TOSs. Over the past 30 years, the overall trend of ESs has been in decline. HQ has continuously deteriorated, especially in areas with rapid urbanization. CS has remained stable, but low-CS areas have gradually expanded, indicating that regional carbon sequestration potential still exists. SDR has fluctuated significantly, reflecting the negative impact of human activities on soil quality. WY has also experienced significant fluctuations, influenced by changes in precipitation, increased evapotranspiration, and inadequate water resource management.

(3) Correlation analysis reveals the dynamic evolution of synergies and trade-offs among ESs. HQ and CS have maintained a strong synergy in most years, while the negative correlation between HQ and WY has gradually intensified, especially in areas experiencing water scarcity. This suggests that, with the progress of urbanization and LUCCs, the competition between ESs, particularly the conflict between water resources and other ecological functions, has become more pronounced, reflecting the profound impact of human activities on ESs. As built-up land expands, the negative trade-offs between ESs become more significant.

(4) This study shows that, in 1992, the HQ, CS, SDR, and WY in the northern and northwestern regions of the Qin-Mang River Basin exhibited significant positive spatial autocorrelation, demonstrating strong synergies. However, by 2022, the ESs in the southern and eastern regions have gradually shown clear trade-offs, with the negative correlations between HQ and CS and between SDR and WY strengthening. This change is primarily attributed to the impact of urbanization on the ecosystem's structure and functions, leading to a reduction in natural land and an increase in conflicts between ESs, especially in resource-limited areas where the mutual constraints among ESs become more pronounced.

Author Contributions: All authors contributed to the study conception and design. Writing and editing: Jiwei Zhao and Luyao Wang; Chart editing: Luyao Wang, Dong Jia and Yaowen Wang; Preliminary data collection: Luyao Wang. All authors have read and agreed to the published version of the manuscript.

Funding: This study was funded by the National Natural Science Foundation of China (51709115), the Henan Provincial Key R&D and Promotion Special Project (Science and Technology Tackling) (182102210066).

Data Availability Statement: Data and materials are available from the corresponding author upon request.

Acknowledgments: The authors would like to thank the anonymous reviewers and the editors for their profound comments, which helped us improve the quality of this paper.

Conflicts of Interest: All authors have read, understood, and have complied as applicable with the statement on "Ethical responsibilities of Authors" as found in the Instructions for Authors.

References

1. Costanza, R.; De Groot, R.; Sutton, P.; Van der Ploeg, S.; Anderson, S.J.; Kubiszewski, I.; Farber, S.; Turner, R.K. Changes in the global value of ecosystem services. *Glob. Environ. Chang.* **2014**, *26*, 152–158. [CrossRef]
2. Chee, Y.E. An ecological perspective on the valuation of ecosystem services. *Biol. Conserv.* **2004**, *120*, 549–565. [CrossRef]
3. Watson, R.; Baste, I.; Larigauderie, A.; Leadley, P.; Pascual, U.; Baptiste, B.; Demissew, S.; Dziba, L.; Erpul, G.; Fazel, A.M.; et al. *Summary for Policymakers of the Global Assessment Report on Biodiversity and Ecosystem Services of the Intergovernmental Science-Policy Platform on Biodiversity and Ecosystem Services*; IPBES Secretariat: Bonn, Germany, 2019; pp. 22–47. Available online: https://pesquisa.bvsalud.org/portal/resource/pt/biblio-1179448 (accessed on 3 August 2024).
4. Li, J.; Xie, B.; Dong, H.; Zhou, K.; Zhang, X. The impact of urbanization on ecosystem services: Both time and space are important to identify driving forces. *J. Environ. Manag.* **2023**, *347*, 119161. [CrossRef] [PubMed]
5. Davidson, N.C. How much wetland has the world lost? Long-term and recent trends in global wetland area. *Mar. Freshw. Res.* **2014**, *65*, 934–941. [CrossRef]
6. Junk, W.J.; An, S.; Finlayson, C.M.; Gopal, B.; Květ, J.; Mitchell, S.A.; Mitsch, W.J.; Robarts, R.D. Current state of knowledge regarding the world's wetlands and their future under global climate change: A synthesis. *Aquat. Sci.* **2013**, *75*, 151–167. [CrossRef]
7. Díaz, S.; Settele, J.; Brondízio, E.S.; Ngo, H.T.; Agard, J.; Arneth, A.; Balvanera, P.; Brauman, K.A.; Butchart, S.H.; Chan, K.M.; et al. Pervasive human-driven decline of life on Earth points to the need for transformative change. *Science* **2019**, *366*, eaax3100. [CrossRef] [PubMed]
8. Long, H.; Liu, Y.; Hou, X.; Li, T.; Li, Y. Effects of land use transitions due to rapid urbanization on ecosystem services: Implications for urban planning in the new developing area of China. *Habitat Int.* **2014**, *44*, 536–544. [CrossRef]
9. Spake, R.; Lasseur, R.; Crouzat, E.; Bullock, J.M.; Lavorel, S.; Parks, K.E.; Schaafsma, M.; Bennett, E.M.; Maes, J.; Mulligan, M.; et al. Unpacking ecosystem service bundles: Towards predictive mapping of synergies and trade-offs between ecosystem services. *Glob. Environ. Chang.* **2017**, *47*, 37–50. [CrossRef]
10. Pang, X.; Nordström, E.M.; Böttcher, H.; Trubins, R.; Mörtberg, U. Trade-offs and synergies among ecosystem services under different forest management scenarios–The LEcA tool. *Ecosyst. Serv.* **2017**, *28*, 67–79. [CrossRef]
11. Yang, J.; Xie, B.; Tao, W.; Zhang, D. Ecosystem services assessment, trade-off, and bundles in the Yellow River Basin, China. *Diversity* **2021**, *13*, 308. [CrossRef]
12. Qiao, Q.; Zhen, Z.; Liu, L.; Luo, P. The construction of ecological security pattern under rapid urbanization in the Loess Plateau: A case study of Taiyuan city. *Remote Sens.* **2023**, *15*, 1523. [CrossRef]

13. Wu, Y.; Zhu, X.; Gao, W.; Qian, F. The spatial characteristics of coupling relationship between urbanization and eco-environment in the Pan Yangtze River Delta. *Energy Procedia* **2018**, *152*, 1121–1126. [CrossRef]
14. Long, K.; Omrani, H.; Pijanowski, B.C. Impact of local payments for ecosystem services on land use in a developed area of China: A qualitative analysis based on an integrated conceptual framework. *Land Use Policy* **2020**, *96*, 104716. [CrossRef]
15. Zhao, Y.; Liu, Z.; Wu, J. Grassland ecosystem services: A systematic review of research advances and future directions. *Landsc. Ecol.* **2020**, *35*, 793–814. [CrossRef]
16. Pontius, G.R.; Malanson, J. Comparison of the structure and accuracy of two land change models. *Int. J. Geogr. Inf. Sci.* **2005**, *19*, 243–265. [CrossRef]
17. Liang, X.; Guan, Q.; Clarke, K.C.; Liu, S.; Wang, B.; Yao, Y. Understanding the drivers of sustainable land expansion using a patch-generating land use simulation (PLUS) model: A case study in Wuhan, China. *Comput. Environ. Urban Syst.* **2021**, *85*, 101569. [CrossRef]
18. Sharp, R.; Tallis, H.; Ricketts, T.; Guerry, A.; Wood, S.A.; Chaplin-Kramer, R.; Nelson, E.J.; Ennaanay, D.; Wolny, S.; Olwero, N.; et al. *InVEST 3.7.0 User's Guide*; The Natural Capital Project: Standford, CA, USA, 2018. [CrossRef]
19. Yang, K.; Han, Q.; de Vries, B. Urbanization effects on the food-water-energy nexus within ecosystem services: A case study of the Beijing-Tianjin-Hebei urban agglomeration in China. *Ecol. Indic.* **2024**, *160*, 111845. [CrossRef]
20. Guo, F.Y.; Liu, X.H.; Zhang, W.B.; Xing, L.Y.; Wang, R.; Zu, P.Y.M.; Luo, X.; Wang, C.; Zhao, H. Spatiotemporal pattern evolution and driving force analysis of habitat quality in the Yellow River Basin (Henan section) from 2000 to 2040. *Mod. Geol.* **2024**, *38*, 599–611.
21. Chen, M.J.; Bai, Z.K.; Wang, Q.R.; Shi, Z. Habitat quality effect and driving mechanism of land use transitions: A case study of Henan water source area of the middle route of the South-to-North Water Transfer Project. *Land* **2021**, *10*, 796. [CrossRef]
22. Feng, J.M.; Li, C.; Feng, Y.F. Evolution of watershed habitat quality based on ISODATA spatial mosaic clustering: A case study of urban areas surrounding the Yellow River Basin in Henan Province. *Chin. Landsc. Archit.* **2024**, *50*, 89–95.
23. Schulte-Uebbing, L.; de Vries, W. Global-scale impacts of nitrogen deposition on tree carbon sequestration in tropical, temperate, and boreal forests: A meta-analysis. *Glob. Change Biol.* **2018**, *24*, e416–e431. [CrossRef] [PubMed]
24. Li, X.; Wang, Y.; Wu, K.; Feng, Z. Analysis and prediction of carbon balance in production-living-ecological space of Henan Province, China. *Environ. Sci. Pollut. Res.* **2023**, *30*, 75973–75988. [CrossRef] [PubMed]
25. Chuai, X.; Huang, X.; Lai, L.; Wang, W.; Peng, J.; Zhao, R. Land use structure optimization based on carbon storage in several regional terrestrial ecosystems across China. *Environ. Sci. Policy* **2013**, *25*, 50–61. [CrossRef]
26. Didoné, E.J.; Minella JP, G.; Merten, G.H. Quantifying soil erosion and sediment yield in a catchment in southern Brazil and implications for land conservation. *J. Soils Sediments* **2015**, *15*, 2334–2346. [CrossRef]
27. Hu, Y.; Tian, G.; Mayer, A.L.; He, R. Risk assessment of soil erosion by application of remote sensing and GIS in Yanshan Reservoir catchment, China. *Nat. Hazards* **2015**, *79*, 277–289. [CrossRef]
28. Feng, X.M.; Sun, G.; Fu, B.J.; Su, C.H.; Liu, Y.; Lamparski, H. Regional effects of vegetation restoration on water yield across the Loess Plateau, China. *Hydrol. Earth Syst. Sci.* **2012**, *16*, 2617–2628. [CrossRef]
29. Jiang, L.; Wang, Z.; Zuo, Q.; Du, H. Simulating the impact of land use change on ecosystem services in agricultural production areas with multiple scenarios considering ecosystem service richness. *J. Clean. Prod.* **2023**, *397*, 136485. [CrossRef]
30. Briner, S.; Huber, R.; Bebi, P.; Elkin, C.; Schmatz, D.R.; Grêt-Regamey, A. Trade-offs between ecosystem services in a mountain region. *Ecol. Soc.* **2013**, *18*. Available online: https://www.jstor.org/stable/26269360 (accessed on 3 August 2024). [CrossRef]
31. Jopke, C.; Kreyling, J.; Maes, J.; Koellner, T. Interactions among ecosystem services across Europe: Bagplots and cumulative correlation coefficients reveal synergies, trade-offs, and regional patterns. *Ecol. Indic.* **2015**, *49*, 46–52. [CrossRef]
32. Tian, S.; Wu, W.; Shen, Z.; Wang, J.; Liu, X.; Li, L.; Li, X.; Liu, X.; Chen, H. A cross-scale study on the relationship between urban expansion and ecosystem services in China. *J. Environ. Manag.* **2022**, *319*, 115774. [CrossRef] [PubMed]
33. Fang, Z.; Ding, T.; Chen, J.; Xue, S.; Zhou, Q.; Wang, Y.; Huang, Z.; Yang, S. Impacts of land use/land cover changes on ecosystem services in ecologically fragile regions. *Sci. Total Environ.* **2022**, *831*, 154967. [CrossRef] [PubMed]
34. Liu, Z.; Chang, Y.; Pan, S.; Zhang, P.; Tian, L.; Chen, Z. Unfolding the spatial spillover effect of urbanization on composite ecosystem services: A case study in cities of Yellow River Basin. *Ecol. Indic.* **2024**, *158*, 111521. [CrossRef]
35. Ouyang, X.; Tang, L.; Wei, X.; Li, Y. Spatial interaction between urbanization and ecosystem services in Chinese urban agglomerations. *Land Use Policy* **2021**, *109*, 105587. [CrossRef]
36. Di Giulio, M.; Holderegger, R.; Tobias, S. Effects of habitat and landscape fragmentation on humans and biodiversity in densely populated landscapes. *J. Environ. Manag.* **2009**, *90*, 2959–2968. [CrossRef] [PubMed]
37. Wang, K.; Ouyang, X.; He, Q.; Zhu, X. Impact of urban land expansion efficiency on ecosystem services: A case study of the three major urban agglomerations along the Yangtze River economic belt. *Land* **2022**, *11*, 1591. [CrossRef]
38. Di Sacco, A.; Hardwick, K.A.; Blakesley, D.; Brancalion, P.H.; Breman, E.; Cecilio Rebola, L.; Chomba, S.; Dixon, K.; Elliott, S.; Ruyonga, G.; et al. Ten golden rules for reforestation to optimize carbon sequestration, biodiversity recovery and livelihood benefits. *Glob. Change Biol.* **2021**, *27*, 1328–1348. [CrossRef]

39. Fu, B.; Zhang, L.; Xu, Z.; Zhao, Y.; Wei, Y.; Skinner, D. Ecosystem services in changing land use. *J. Soils Sediments* **2015**, *15*, 833–843. [CrossRef]
40. Luo, Q.; Zhou, J.; Zhang, Y.; Yu, B.; Zhu, Z. What is the spatiotemporal relationship between urbanization and ecosystem services? A case from 110 cities in the Yangtze River Economic Belt, China. *J. Environ. Manag.* **2022**, *321*, 115709. [CrossRef]
41. Gong, J.; Dai, X.; Wang, L.; Niu, Z.; Cao, Q.; Huang, C. The Impact of Urbanization on the Supply–Demand Relationship of Ecosystem Services in the Yangtze River Middle Reaches Urban Agglomeration. *Remote Sens.* **2023**, *15*, 4749. [CrossRef]
42. Liu, T.; Yu, L.; Chen, X.; Wu, H.; Lin, H.; Li, C.; Hou, J. Environmental laws and ecological restoration projects enhancing ecosystem services in China: A meta-analysis. *J. Environ. Manag.* **2023**, *327*, 116810. [CrossRef] [PubMed]
43. Seppelt, R.; Lautenbach, S.; Volk, M. Identifying trade-offs between ecosystem services, land use, and biodiversity: A plea for combining scenario analysis and optimization on different spatial scales. *Curr. Opin. Environ. Sustain.* **2013**, *5*, 458–463. [CrossRef]